Review

Review of Recent Developments in the Formulation of Graphene-Based Coatings for the Corrosion Protection of Metals and Alloys

Bronach Healy, Tian Yu, Daniele da Silva Alves and Carmel B. Breslin *

Department of Chemistry, Maynooth University, Maynooth, Co. Kildare, Ireland;
bronach.healy.2017@mumail.ie (B.H.); Tian.Yu.2020@mumail.ie (T.Y.); danicosta.0607@gmail.com (D.d.S.A.)
* Correspondence: Carmel.Breslin@mu.ie

Abstract: Corrosion is a naturally occurring phenomenon and there is continuous interest in the development of new and more protective coatings or films that can be employed to prevent or minimise corrosion. In this review the corrosion protection afforded by two-dimensional graphene is described and discussed. Following a short introduction to corrosion, the application of graphene in the formulation of coatings and films is introduced. Initially, reduced graphene oxide (rGO) and metallic like graphene layers are reviewed, highlighting the issues with galvanic corrosion. Then the more successful graphene oxide (GO), functionalised GO and polymer grafted GO-modified coatings are introduced, where the functionalisation and grafting are tailored to optimise dispersion of graphene fillers. This is followed by rGO coupled with zinc rich coatings or conducting polymers, GO combined with sol-gels, layered double hydroxides or metal organic frameworks as protective coatings, where again the dispersion of the graphene sheets becomes important in the design of protective coatings. The role of graphene in the photocathodic protection of metals and alloys is briefly introduced, while graphene-like emerging materials, such as hexagonal boron nitride, h-BN, and graphitic carbon nitride, g-C$_3$N$_4$, are then highlighted.

---

1. Introduction

Corrosion is a naturally occurring phenomenon that results in the oxidation of metals or alloys and this is normally accompanied by dissolution of the metal or alloy. It can affect the performance of materials used in many technological fields, ranging from light-weight aluminium alloys employed in the aerospace industry [1], metals and alloys used in the electronics industry [2], transportation [3], pipeline [4], wastewater treatment [5], coatings and linings for food storage [6], pulp and paper [7], fuel cells [8] and refining industries [9]. Many of the traditional corrosion protective strategies, for example, those employing chromates, especially hexavalent chromium [10], are no longer viable due to environmental considerations. Consequently, there is an ever-increasing interest in developing new and environmentally acceptable corrosion-control technologies.

The corrosion reaction can be represented as two half-cell reactions, with the oxidation reaction corresponding to the oxidation of the metal, M, Equation (1), while the reduction reaction, which consumes the electrons, is typically the reduction of oxygen at neutral pH values, Equation (2), or under acidic conditions, the reduction of H$^+$ becomes the predominant reaction, Equation (3).

$$M \rightarrow M^{n+} + ne^- \tag{1}$$

$$O_2 + 4H^+ + 4e^- \rightarrow 2H_2O \tag{2}$$

$$2H^+ + 2e^- \rightarrow H_2 \tag{3}$$
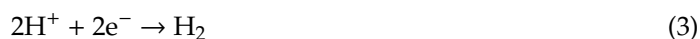
The sites for the oxidation reaction are termed anodic sites, while the reduction reactions occur at cathodic sites on a surface. These anodic and cathodic sites can be spatially separated and fixed at locations, such as heterogeneities or defects on the surface. This normally leads to localised corrosion, such as pitting, crevice, intergranular or galvanic corrosion [11]. A schematic representation of pitting corrosion is shown in Figure 1a. This localised attack gives rise to the formation of deep pits, Figure 1c, while the pit contents are acidified as a result of hydrolysis reactions. Alternatively, if the cathodic and anodic sites fluctuate randomly across the surface, then uniform or nearly uniform corrosion is generally observed as illustrated in Figure 1b. These corrosion reactions will propagate with the oxidation reaction, Equation (1), and reduction reaction, Equations (2) or (3), occurring until the conducting path is interrupted and this is one way in which the corrosion reaction can be halted.
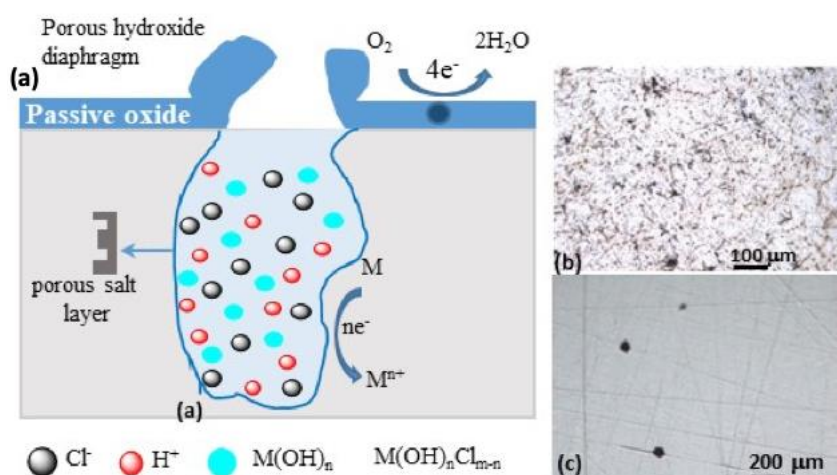

Figure 1. (**a**) Schematic representation of pitting attack and micrographs illustrating (**b**) general-like dissolution and (**c**) pitting attack.

Various coatings and surface modifications have been applied to limit this conducting pathway and protect the underlying substrate. These approaches include the deposition of metallic coatings or composites [12], polymeric coatings [13] and conversion coatings [14]. Electroplating is a well-known and versatile method for forming metallic coatings and this approach is applicable to any system that can be electrochemically reduced from the ionic to the metallic state when present in the electrolyte solution [15]. However, certain metals such as aluminium, titanium and magnesium cannot be electrodeposited from aqueous solutions as the competing hydrogen ion reduction reaction is thermodynamically favoured and will occur in preference to the reduction of the metal ions. Nevertheless, this can be achieved in ionic liquids or in conducting organic electrolytes where the hydrogen ion reduction reaction is negligible [16]. Polymeric coatings, which include paints, lacquers and varnishes, normally protect the substrate from corrosion by acting as a barrier, preventing the reactants, water, oxygen and ions, from reaching the protected substrate. The protective properties of these coatings typically improve as the thickness of the coating is increased, while fillers and pigments can be added to increase the diffusion path for water and oxygen. Conversion coatings is the term used to describe coatings where the substrate takes part in the coating formation reactions, with the best known being the commercial phosphate conversion coatings.

In more recent years, there has been considerable interest in using graphene to provide corrosion protection and it has been employed to provide protective metallic coatings or composites and also added to various polymeric coatings. The level of interest in graphene in the field of corrosion science is readily evident from Figure 2, with the number of publications increasing each year. Graphene

with six-membered carbon rings, arranged as single-, bi- or a few sheets, is a two-dimensional (2D) material that has attracted considerable interest [17]. Since its discovery, it has found applications as sensors [18,19], in batteries [20], electro-Fenton [21,22], electronics [23], capacitors [24] and in energy storage [25]. This is not surprising as it has very good electronic, optical, magnetic, thermal and mechanical properties, combined with excellent stability and a high surface area. Graphene-based materials are readily synthesised by forming graphene oxide (GO) from the oxidisation of graphite using the well-known modified Hummers method [26–28]. The interlayer spacing increases as the graphite is oxidised and exfoliation is achieved through ultrasonication to give GO sheets. While these sheets can be reduced using various reducing agents, such as borohydride or the more environmentally acceptable ascorbic acid at room temperature [29] or through electrochemical reduction [30–32], the complete reduction of GO to rGO is difficult to achieve. Consequently, the rGO will inevitably have some oxygen-containing functional groups. While rGO is finding applications in the formulation of metallic-like corrosion protective coatings, the more insulating GO is being employed more widely, making use of its oxygen-containing functional groups.
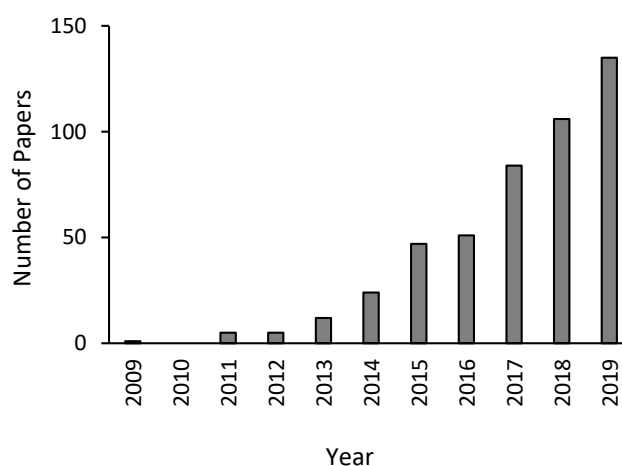

Figure 2. Summary of the number of graphene-based papers published in recent years on corrosion protection, taken from Scopus.

In this review paper the applications of 2D graphene flakes or sheets, including rGO and GO, and graphene-like 2D materials, such as boron nitrides and graphitic carbon nitrides, in corrosion protective films and coatings is reviewed and discussed. There have been a number of review articles that describe graphene-based coatings, including a review by Nine et al. [33] in which the antifouling, pollutant adsorption, flame retardant and protective graphene-based coatings are discussed, while Ding et al. [34] have briefly reviewed graphene and graphene oxide in the field of corrosion protection, Othman et al. [35] have reviewed the utilisation of graphene in the formulation of polymer matrices for barrier coatings, Ding et al. [36] have described graphene-modified anticorrosion organic coatings, Cui et al. [37] have reviewed graphene-based anticorrosive coatings, while graphene-based metal matrix composite coatings have also been reviewed [38]. In this review paper, we include and discuss a broad range of graphene-based corrosion protective films and coatings, including graphene-modified epoxy coatings, sol-gel films, double-layered hydroxides, conducting polymers, zinc-rich coatings and metallic-like coatings, while the role played by graphene-like materials, such as 2D hexagonal boron nitride and graphitic carbon nitride are also included.

2. Graphene-Based Metallic-Like Coatings

Graphene-based metallic or GO coatings can be deposited using a variety of methods including chemical vapour deposition [39], spin coating [40], graphene-based inks [41,42] and electrophoretic deposition [43,44], with the latter attracting considerable attention in the formulation of graphene-based

coatings for the protection of corrosion susceptible metals or alloys [45]. It is based on the migration of electrostatically charged particles to an oppositely charged electrode under an electric field. The charged particles deposit onto the electrode to form a dense and homogeneous coating. Typically, GO or rGO sheets are suspended in a solution to give negatively charged particles or sheets which are deposited at the anode of the cell. However, it is also possible to generate positively charged GO particles enabling cathodic deposition of the particles by using various salts [46,47], *p*-phenylenediamine [48] or by altering the pH to values in the vicinity of 2.0, which are below the isoelectric pH of rGO [49]. The performance of various electrophoretic graphene-based protective coatings is illustrated in Table 1, where the corrosion current density, j_{corr}, and corrosion potential, E_{corr}, for the bare and graphene-modified surfaces are compared. These parameters provide details on the extent of the corrosion event, with j_{corr} being a measure of the rate of the corrosion reaction and E_{corr} a thermodynamic factor. The j_{corr} value cannot be measured directly and instead it is estimated from a Tafel plot, where the applied potential is plotted as a function of the logarithm of the measured current. A schematic plot is shown in Figure 3a, where the linear regions of the anodic and cathodic branches are extended and intersected to give the computed j_{corr} and E_{corr} values. The principle of this mixed-potential theory is illustrated in Figure 3c, where the corrosion reaction can be algebraically divided into separate oxidation and reduction half reactions with no net accumulation of electrical charge. As a consequence, the rate of the oxidation reaction is equal to the rate of the reduction reaction. As illustrated in Figure 3b the j_{corr} value is lowered and E_{corr} adopts more positive values when the anodic metal dissolution reaction is inhibited. Likewise, if the reduction half reaction is lowered in magnitude, then j_{corr} is decreased, but E_{corr} reaches more negative values. Consequently, these estimated parameters are sensitive to the rates of the two half reactions during the corrosion event. The corresponding Butler–Volmer equation is provided in Equation (4), where α and β are the transfer coefficients of the cathodic and anodic half-reactions, respectively, while the Tafel relationships are illustrated in Equations (5) and (6).

$$j = j_{corr}\left(e^{-\alpha(E-E_{corr})F/RT} - e^{\beta(E-E_{corr})F/RT}\right) \tag{4}$$

$$E - E_{corr} = \frac{2.303RT}{\alpha F}\log j_{corr} - \frac{2.303RT}{\alpha F}\log j \tag{5}$$

$$E - E_{corr} = -\frac{2.303RT}{\beta F}\log j_{corr} + \frac{2.303RT}{\beta F}\log j \tag{6}$$

As evident in Table 1, there are a number of reports which clearly show that the j_{corr} value is decreased and the E_{corr} value is increased on application of the graphene-based coating through either electrophoretic deposition (EPD), from a slurry, inks or by chemical vapour deposition (CVD), indicating a lowering of the corrosion rate. These corrosion measurements were made in different aqueous solutions and therefore a comparison between the studies is difficult; however, on comparing the pristine untreated and graphene-modified substrates, the corrosion protection afforded by the deposited graphene-based coatings is clearly evident, at least for short periods.

Despite the promising findings summarised in Table 1, the role of graphene as a corrosion inhibition coating is often disputed, especially its long-term performance. For example, graphene-based coatings on copper have shown good long term stability in humid environments for up to 1.5 [50] or 2.5 years [51] and Scardamaglia et al. [52] have shown that graphene-based coatings act as effective barriers at high temperatures and prevent the corrosion of the underlying copper. However, it has also been argued that the oxygen trapped during formation of the graphene-based layers gives rise to oxidation of the copper substrate [53], while Schriver et al. [54] have demonstrated that graphene promotes more extensive corrosion than that observed with the uncoated copper over a long-term period. The authors proposed a mechanism whereby the diffusion of oxygen and water through graphene defects gives rise to corrosion across the entire copper substrate, with the conducting graphene maintaining electrical contact and facilitating the corrosion reactions. Moreover, as rGO is conducting, galvanic corrosion becomes possible. While the electrode potential adopted by graphene or graphite depends on its surface

chemistry and extent of oxidation, it has been reported as approximately 0.15 V vs. SCE [55], making it significantly more positive than the corresponding potentials adopted by various corrosion susceptible metals or alloys. Therefore, as the electrolyte permeates through the graphene-based coating, a galvanic corrosion cell is established leading to enhanced corrosion. It has also been suggested that chloride ions can accumulate at graphene edges [54] and these aggressive anions promote dissolution. Moreover, the adhesion of graphene to certain metal substrates, such as Al and its alloys [56], limits its ability to enhance the corrosion resistance of these materials. Various strategies have been employed in an attempt to enhance the adhesion between the graphene-based layer and the aluminium substrate, such as annealing of the GO layers or spin coating [56] or the utilisation of molecules such as fulvic acid [40] or polyvinyl alcohol (PVA) [57] which act as binders between Al and GO or rGO.
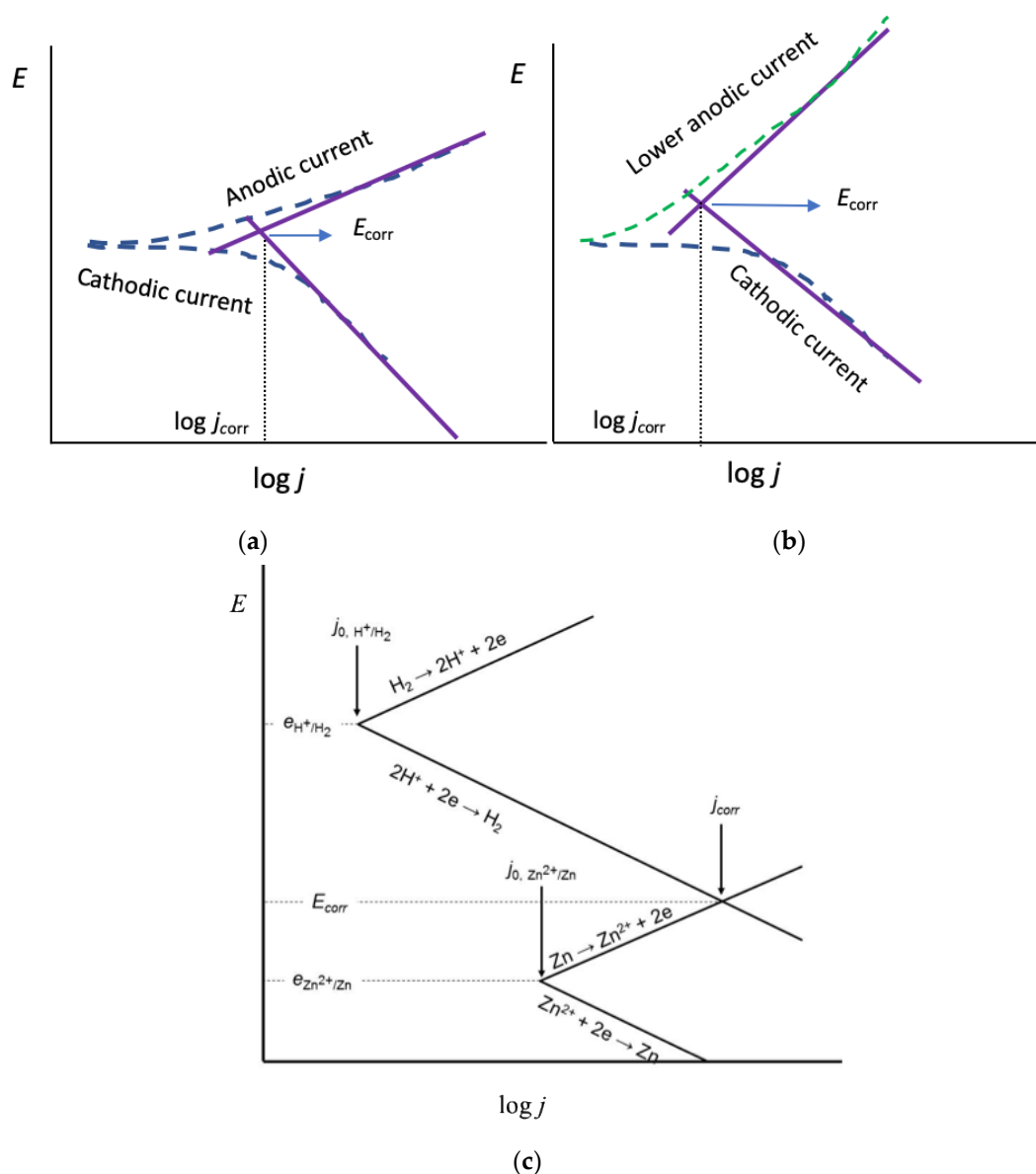
Figure 3. Schematic diagram of a Tafel plot illustrating the estimation of j_{corr} and E_{corr} with (**a**) depicting a mixed corrosion event and (**b**) an inhibited corrosion event with lower anodic dissolution currents and (**c**) Evans diagram, depicting the $H^+|H_2$ and $Zn^{2+}|Zn$ couples and the mixed corrosion reaction. The dashed traces in (**a**,**b**) correspond to measured data, while the solid traces show the linear Tafel regions, fitted to the experimental data.

Table 1. Summary of the performance of deposited G, GO or rGO films in corrosion protection.

System	Deposition Conditions	E_{corr}/mV	j_{corr}/μA cm^{-2}	Ref
Cu	EPD 20.0 V/60 s	−211	25.0	[58]
GO/Cu		−195	12.7	
Steel	EPD 4.0 V		1.47	[59]
GO/steel		−	0.095	
Fe	EPD 2.3 V/60 min	−0.57	3.01	[60]
GO/Fe (GO flakes, 20 ± 5 μm)		−0.42	2.01	
Carbon Steel		−444	77.7	
Ni	EPD 100 mA cm^{-2}	−412	63.2	[49]
rGO/Ni coated carbon steel		−343	4.23	
CuNi		−37	1.66	
GO/CuNi	−	90	2.92	[61]
GO/acrylic polymer-CuNi		220	0.003	
CuNi	EPD 10 V/60 s	−36	8.56	[62]
GO/chitosan-Ag Cu-Ni		30	1.10	
NiTi		−170	0.158	
GO/NiTi	EPD 10 V/10 min	31	0.017	[63]
GO/Ag-NiTi		8	0.002	
Ti6Al4V	EPD 50 V/5 min	−395	0.143	[64]
GO/Ti6Al4V		−205	0.032	
Mild steel (MS)		−692	650	
rGO-MS	Slurry deposition	−420	0.0051	[65]
rGO/TiO$_2$-MS		−386	0.0028	
SS	Ball milling	−407	5.5	[66]
GO/SS		−284	0.3	
Cu (annealed)	CVD	−388	90.1	[39]
G/Cu (annealed in 20% H$_2$)		−239	0.15	
GO/Al	Spin coating	−426	9.54	[40]
G/FA-Al		−548	0.84	
CS	GO ink	−714	9	[42]
CS/GO		−474	0.00065	

Abbreviations: EPD, electrophoretic deposition; CS, carbon steel; SS, stainless steel; FA, fluvic acid; CVD, chemical vapour deposition.

As the corrosion protection performance of conducting graphene-based coatings remains debated and controversial, an alternative avenue of research has developed and this is based on the incorporation of graphene flakes or sheets within various polymer matrices. In this case if the graphene sheets can be well dispersed and aggregation prevented then direct electrochemical coupling with the metal substrate can be avoided.

3. Graphene as a Nanofiller in Non-Conducting Anti-Corrosion Coatings

There has been considerable interest and progress made in the development of anti-corrosion coatings such as epoxy, polyurethane, phenolic and various resin-based coatings. They have excellent barrier protection, preventing water and ions from reaching the substrate, coupled with very good adhesion properties. However, micro-cracks can appear in these coatings during their service life, as they become damaged in their environments and consequently the substrate is no longer protected from corrosion events. Various fillers have been employed and embedded into these coatings in an attempt to enhance the corrosion protection properties and in particular the long-term corrosion protection. Nanofillers such as nano-sized particles, including TiO$_2$ [67], Al$_2$O$_3$ [68], SiO$_2$ [69] and clay particles [70] have been employed, while graphene-based additives are being used increasingly and combined with other fillers in an attempt to enhance the protection of these anti-corrosion coatings.

A number of different approaches has been used to incorporate graphene as a nanofiller, including the simple dispersion of GO within the coating [71], the introduction of functional groups to give functionalised GO to aid dispersion within the coating [72], grafting of the polymer onto the GO surface [73] and incorporation of GO with other nano-sized fillers, such as SiO$_2$/GO [74] or Al$_2$O$_3$-GO [75]. Both GO and rGO have been used to form protective epoxy composites and it has been shown that better anti-corrosion properties are observed when GO is combined with a non-electroactive epoxy, while rGO performs well when used in combination with an electroactive epoxy thermoset [76].

Dutta et al. [77] have argued that electrochemically exfoliated graphene is the best choice of filler and that by tailoring the amount and size of the graphene flakes within hydrophobic and water borne polymer composites, galvanic corrosion between the underlying substrate and graphene can be avoided. It has also been shown that the size of the GO flakes can have a significant effect on the dispersion, mechanical and anti-corrosion performance of coatings [78], while the aspect ratio of GO can also influence its dispersion in epoxy and resins, with higher aspect ratios giving greater corrosion protection [79]. While well-dispersed GO can be utilised to form protective coatings, this approach suffers from the inevitable aggregation of the GO sheets and this can result in relatively poor long term corrosion protection. In the last decade efforts have been made to alleviate these issues and these are now described below.

3.1. Functionalized GO

While the exact structure of GO depends on how it is synthesised and its level of oxidation, it is well known that hydroxyl, carboxyl, carbonyl, phenol, epoxy, lactone and quinone groups are present, with the epoxy and hydroxyl groups residing on the basal plane, and carboxyl, lactone, phenol, carbonyl and quinone groups at the edges of the sheets [80]. These oxygenated groups can be further employed to chemically modify the GO sheets with different functionalities. For example, one of the earliest chemical modifications of GO involved activating the carboxylic groups through nucleophilic addition reactions [81]. Likewise, the epoxy group undergoes ring opening reactions and this can be exploited to functionalise GO with an amide or ester group. With these advances in the chemical functionalisation of GO, it is now possible to add various groups to GO to aid its dispersion in anti-corrosion coatings.

Various functionalised GO sheets have been incorporated into epoxy coatings with the aim of enhancing the dispersion of the sheets and increasing the corrosion protection properties of the coatings. For example, it has been shown that the introduction of polyvinylpyrrolidone reduced GO (PVP-rGO) into an epoxy resin coating leads to a significant increase in the Young modulus, thermal stability and corrosion protection [82]. In other studies, GO has been functionalised with hydroxyl-terminated hyper-branched polyamide [83], poly(o-phenylenediamine) [84], trialkoxysilane [85], triethoxysilane [86], maleic anhydride [87], ammonium [88] and a cyclodextrin, β-CD [89] and then incorporated within the epoxy coating. In all these studies, it has been show that the addition of the functionalised GO enhances the protective properties of the epoxy coating and this enhanced corrosion resistance has been attributed to an increase in the barrier protective properties of the coating, inhibition of the diffusion of oxygen and ions to the substrate, good dispersion of the functionalised GO, the hydrophobic properties of GO, an increase in the ionic resistance of the coating and reduction in the pore sizes within the coating.

In Table 2 the protective properties of some epoxy coatings modified with functionalised GO fillers is summarised where the coating resistance, R_c, and coating capacitance, C_c, are shown. These parameters and indeed detailed information on the corrosion protection properties of these coatings are normally studied using electrochemical impedance spectroscopy (EIS). In the classical EIS experiment the input signal is an alternating voltage and the output signal is the corresponding alternating current with the same frequency and different phase. The ratio of the sinusoidal voltage to sinusoidal current gives the impedance, Z. A simulated Nyquist plot is shown in Figure 4 where a coating with a single-time constant, typical of a protective coating, is compared with a two-time constant system, which indicates the onset of substrate dissolution. This emergence of a second time constant is a very convenient way to monitor the protective properties of a coating. Using EIS it is also possible to discern between different processes depending on their time scales, with slow processes such as the diffusion of ions through a protective polymer coating appearing at low frequencies. Therefore, changes in the impedance at low frequencies, such as 0.01 to 0.05 Hz, can be attributed to diffusion processes that will limit the barrier protective properties of coatings. This is illustrated by a decrease in the impedance at low frequencies as illustrated in Figure 4b, or alternatively changes in the

equivalent circuit elements can be followed and related with the protective properties of the coatings in various environments. Moreover, the extent of delamination can be estimated by monitoring the breakpoint frequency (frequency at −45° phase angle). As the electrolyte diffuses into the polymer and corrosion occurs at the polymer substrate interface delamination of the coating can occur and this gives rise to higher breakpoint frequencies [90,91].

Table 2. Anti-corrosion properties of functionalised graphene containing epoxy coatings.

| Substrate	System	Coating/µm	R_c/kΩ cm²	C_c/µF	Ref
Q 235 steel	Lignin/OH/GO	50 ± 5	28	−	[92]
Mild steel	Gelatin/GO	35.7 ± 0.5	6.0	2.8×10^{-4}	[93]
Carbon steel	Sulfonated/GO	15	389	1.4×10^{-3}	[72]
Mild steel	Aminothiazole/GO	23.5 ± 0.5	101	0.26	[94]
Mild steel	Amino-naphthyl thiazole/GO	23.5 ± 0.5	6.5×10^4	0.15	[94]
Q 235 steel	Phytic acid/GO	−	−	−	[90]
Mild steel	Amino/GO	−	7.3×10^6	8.0×10^{-4}	[91]
Steel	Aminopropyltriethoxysilane/GO	50 ± 5	4.8	53	[95]
Mild steel	Amino-silane modified/GO	150 ± 10	1×10^4	−	[96]
Steel	L-histidine/GO	30 ± 3	1×10^8 (0.01 Hz)	−	[97]
Steel	L-cysteine/GO	60 ± 5	28	47.9	[98]
Mg AZ31	Leucine/GO	−	38 Ω	2.7	[99]
Steel	Polyamidoamine dendrimer/GO	60 ± 5	270	2.34	[100]
Mg alloy	Polydopamine and hydroxyquinoline/GO	−	14.3	2.4×10^{-4}	[101]
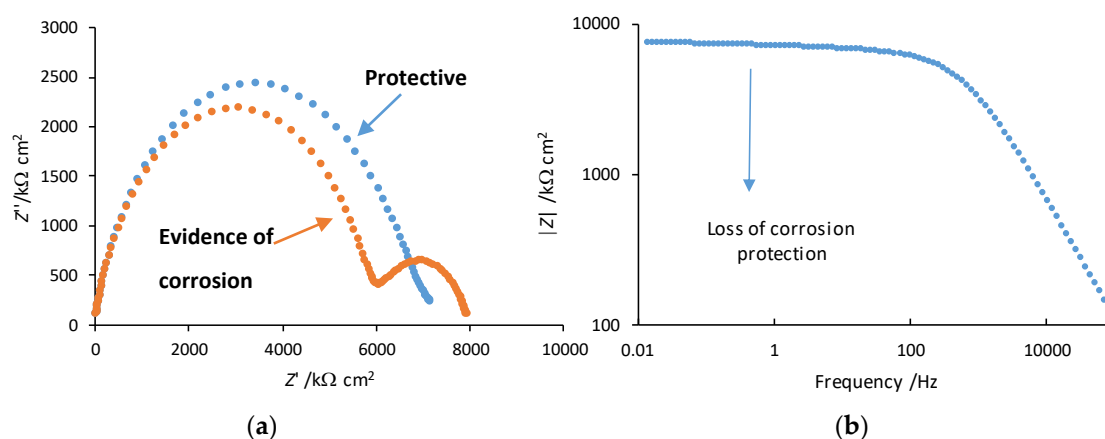
Figure 4. Simulated impedance data. (**a**) Nyquist diagram illustrating a protective coating (blue) and the onset of substrate dissolution (orange) and (**b**) Bode plot typical of a protective coating.

In addition to epoxy coatings, other polymeric systems have been employed with GO and functionalised GO as corrosion protective coatings, with polyurethane composites [102,103] being one of the more popular following the epoxy-based system. Polyurethane composites have been modified with amine functionalised GO [104], GO functionalised with dodecylbenzenesulfonate [105], isocyanate [106], 3-aminopropyltriethoxysilane (APTES) [107], two-branched dioctylpyrophosphate and three-branched dioctylpyrophosphate [108], polydopamine [109] and triethylene tetramine-polyethylene glycol diglycidyl ether [110]. In all these cases, good corrosion protection was achieved. In addition, a polycaprolactone polymer modified with functionalised GO was utilised to protect mild steel [111], while silicylacrylate core-shell copolymers [112] and beeswax/GO nanocomposites [113] have also been successfully employed.

In an attempt to further enhance the corrosion protection afforded by these coatings corrosion inhibitors have been added to the coatings. GO is well known as an adsorbent [114] and it has been employed as a nanocontainer to load corrosion inhibitors into epoxy-based coatings. These systems are interesting because they have the potential to act as a self-healing system, releasing the inhibitor at a corrosion site and increasing the service life of the coating. Javidparvar et al. [115] employed this approach to deliver cerium and benzimidazole inhibitors to give

a self-healing epoxy coating, while metronidazole [116], 8-hydroxylquinoline [117], phosphate [118], 1H-benzimidazole [119], trivalent-cerium ions [98], benzotriazole [120,121], aspartic acid [122], benzimidazole-zinc phosphate [123], 2-mercaptobenzothiazole (MBT) [124], zinc acetylacetonate [125] and molybdate [126] have also been adsorbed onto GO and employed as the corrosion inhibitors.

3.2. Polymer Grafted GO

This is one of the most efficient ways of introducing GO into anti-corrosion coatings, but also time consuming in terms of the synthetic reactions. This approach enables the true integration of the properties of GO and the polymer or coating, while the abundant functional groups on GO, which include carboxyl, epoxy and hydroxyl, can be easily employed to provide linkages between the polymer and GO [127,128]. Moreover, using this approach the grafted GO can be homogenously dispersed in polymeric dense matrices, giving very good interfacial adhesion while minimising aggregation issues [129]. A variety of chemical reactions can be employed to graft polymer chains onto GO sheets. A schematic of this grafting approach is illustrated in Figure 5, where the GO is initially functionalised with the required groups, followed by grafting of the polymer and finally the polymer-grafted GO is mixed with epoxy and cured to give the final coating. For example, Xie et al. [73] have employed a free radical polymerisation reaction (RFP) to graft polyacrylate onto GO sheets with the aim of increasing the dispersion of GO within an epoxy coating and as shown in Table 3, this approach gives rise to highly protective coatings with little evidence of any loss in corrosion protection over a 40-day period. An atom-transfer radical polymerisation reaction (ATRP) was used by Qi et al. [130] to graft poly(methylmethacrylate) chains onto GO sheets, while Jiang et al. [131] grafted polyethylenimine (PEI) onto the GO surface to form polymer-GO/epoxy coatings. In another recent study, PAM100, which is a commercially available acrylate ester that undergoes free radical polymerisation reactions, was grafted to GO using a Michael addition click reaction [132]. Initially, the GO was modified with γ-mercaptopropyl triethoxysilane to create a thiol-capped GO which can act as the precursor for the click addition reaction. The thiol-capped GO was then chemically grafted to PAM100 using a Michael addition click reaction. The resulting PAM100-modified GO, when combined with waterborne epoxy, gave a homogenous distribution of PAM100-GO within the epoxy coating. This eliminated aggregation of the GO sheets to give enhanced corrosion protection. In all cases, the polymer-grafted GO/epoxy composite coatings had greater corrosion protection properties and longer service life compared to the GO/epoxy system. In Table 3, various polymer-grafted GO coatings employed in corrosion protection are summarised. In all cases, these provide very good corrosion protection properties and appear to be especially effective in protecting substrates for extended periods.
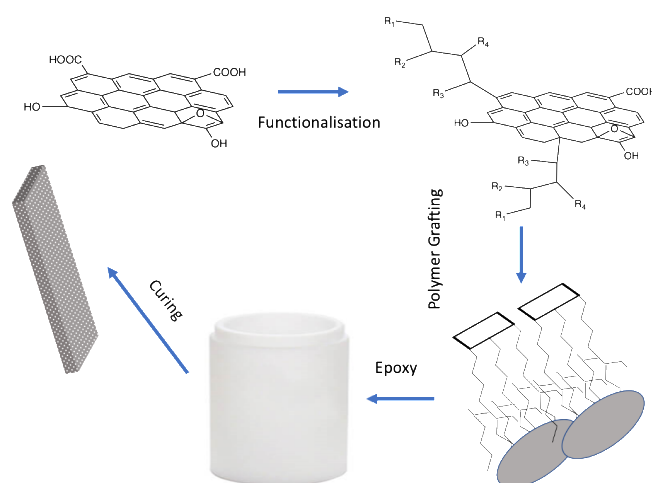

Figure 5. Schematic illustrating the functionalisation of GO sheets followed by grafting to a polymer, combined with epoxy and cured to give the final coated electrode.

Table 3. Anti-corrosion properties of grafted GO epoxy polymer coatings.

System	Time/Days	Filler/wt%	Rc/kΩ cm^2	Ref
	1		1.80×10^7	[73]
GO/epoxy	20		5.50×10^6	[73]
	40	0.1	1.60×10^5	[73]
	1		1.45×10^7	[73]
Polyacrylate/GO/epoxy	20		5.05×10^7	[73]
	40		1.50×10^7	[73]
Acrylamide/acrylic functionalised GO composites/Mg	–	–	53	[133]
	1 h		3.75×10^4	[130]
Polymethylmethacrylate (PMMA) brushes on GO	5 h		3.45×10^4	[130]
	10 h	–	0.99×10^3	[130]
	100 h		1.4×10^2	[130]
	1		6.62×10^3	[132]
PAM100/GO/epoxy	20	0.5	6.12×10^3	[132]
	40		4.63×10^3	[132]

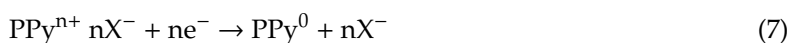## 4. Graphene Combined with Conducting Polymers

Conducting polymers, such as polypyrrole (PPy) and polyaniline (PANi), are readily synthesised through the electropolymerisation of the corresponding monomers [134]. They have been formed at various corrosion susceptible metals and alloys and have been shown to give good corrosion protection, especially for short periods of time (typically weeks) [135,136]. It has been shown in a number of studies that conducting polymers, such as polypyrrole, can be used as intercalators to achieve good dispersion of the graphene sheets, while the conducting/semiconducting properties of the pristine graphene, rGO or GO counterparts are retained. These polymers attach to the basal plane through non-covalent $\pi-\pi$, lone pair$-\pi$ and H-bond interactions to stabilise the graphene-polymer composite, while the very good affinity of these conducting polymers towards GO stems from H-bond interactions between the pyrrole subunits and epoxy groups [137].

PPy/graphene or PPy/GO can be formed by oxidising the pyrrole monomer in the presence of graphene to give nanocolloids that can then be applied to a surface [138] as a coating, used as a filler in the formulation of composite coatings [139], or the monomer can be electropolymerised in the presence of GO to give a PPy/GO composite coating [140]. These three approaches have been used to form corrosion protective coatings. For example, Jiang et al. [140] formed polypyrrole doped with GO, while Li et al. [141] used a similar electropolymerisation process and then the coating was electrochemically reduced to give PPy/rGO. The corrosion protection efficiency, obtained from a comparison of the corrosion current densities of the coated and un-coated carbon steel substrate, was computed as 95.9%. In an earlier study, graphene was deposited onto Cu foils using CVD and then polypyrrole was electrodeposited in order to seal the defects in the graphene layer [142]. These conducting polymer coatings are particularly suited for applications in fuel cells where corrosion protection is required but bipolar plates must also exhibit conductivity. Indeed, in a recent study a bilayer coating, comprising an inner layer of PPy/GO designed to enhance adhesion of the coating and an outer layer of polypyrrole doped with camphorsulfonic acid aimed at enhancing the conductivity of the coating, was employed to protect SS304 bipolar plates in a proton exchange membrane fuel cell [143]. Epoxy coatings have also been modified with PPy/graphene and PPy/GO nanocolloids to give enhanced corrosion protection to the coatings [139,144], while zinc phosphate, well known for its corrosion inhibition properties and sacrificial protection [145], has been combined with these nanocolloids to give enhanced passivation [146]. In these studies, the good corrosion protection is attributed to the very good dispersion of the graphene flakes with polypyrrole acting as an intercalator, the good barrier protection of the coating, while the redox properties of polypyrrole facilitate the formation of passive oxide layers.

Similarly, PANi has been combined with graphene with the aim of increasing the dispersion of the graphene sheets to give corrosion protective coatings. These conducting polymer films have been formed through the electropolymerisation of aniline in the presence of well dispersed GO sheets to give

protective coatings for aluminium alloys [147,148], iron [149] and a magnesium alloy [150]. There have also been a number of publications devoted to the incorporation of PANi and graphene into epoxy coatings [151–156] and in all these coatings good corrosion protection has been achieved. In addition, the corrosion inhibitors benzotriazole [157] and tannic acid [158] have been added to PANi/GO epoxy coatings to provide a self-healing effect by releasing the inhibitors when the coating is damaged locally, while zinc-rich PANi/GO epoxy coatings have been formulated and successfully used in corrosion protection [159,160]. Other combinations include PAni/CeO$_2$ grafted GO nanosheets [31], GO/PANi modified by polydopamine and incorporated within a water-based alkyd varnish [161], while shorter chain aniline trimers [162,163], tetramers [164] and water-soluble carboxylated aniline trimers [165] have been employed rather than PANi to act as an intercalator for graphene aiding its dispersion in the epoxy coating.

The corrosion protection afforded by these GO-modified conducting composites has been attributed to efficient dispersion and a corresponding reduction in the aggregation of the graphene flakes, GO or rGO, greater adhesion coupled with good barrier protective properties with compact films that limit the inward diffusion of ions and O$_2$. For the in situ electropolymerised polymers, the GO, with carboxylic acid groups, can serve as an anionic dopant that will be difficult to expel at local corrosion sites where the polymer is reduced. With small dopants (X$^-$) the reduction of polypyrrole gives rise to the release of the dopant ion, Equation (7), but as illustrated in Equation (8), the GO dopant (GO-COO$^-$), remains largely immobile with the incorporation of cations, M^{m+}, to maintain charge balance. This minimises the uptake of aggressive anions, such as Cl$^-$, that promote corrosion attack.

$$PPy^{n+} \, nX^- + ne^- \rightarrow PPy^0 + nX^- \tag{7}$$

$$PPy^{n+}nGO\text{-}COO^- + ne^- \rightarrow PPy^0nGO\text{-}COO^-(n/m)M^{m+} \tag{8}$$

It has been shown that cation transport in anion-doped polypyrrole is fast, as the cations can hop between adjacent fixed negative charges [166] and while this will prevent the uptake of aggressive anions, the ingress of Na$^+$ and its associated solvated water molecules can lead to structural damage within the polypyrrole matrix [167]. In addition, the PPy/GO coating can shift the potential of the substrate into the passive domain with the formation of protective oxides, the so-called anodic protection mechanism [168]. As long as the passive oxides remain intact and stable, corrosion is inhibited; however, if a local event such as pitting attack occurs at the oxide covered substrate then the rate of attack can be very high, ultimately leading to coating delamination.

5. Graphene Multilayers Combined with Polymers

Layered and multi-layered graphene-containing composites with tunable properties have attracted considerable interest in electromagnetic field absorption [169] and more recently they have been employed as corrosion protective coatings [170–173]. In earlier studies, a single layer of graphene was employed in the multi-layered coatings. For example, Fan et al. [170] formed self-healing anti-corrosion coatings for the protection of a magnesium alloy using an initial cerium-based conversion coating, followed by a layer of GO and then layers of a branched poly(ethylene imine)/poly(acrylic acid). However, in more recent studies higher numbers of graphene layers have been employed and this appears to improve the corrosion protection properties. In a recent study, a multi-layered epoxy resin coating was formed using a stepwise coating method, whereby alternating layers of graphene/epoxy and alumina/epoxy were employed [171]. Good corrosion protection was achieved and this was attributed to the interface between the alternating multilayers, which imped the movement of the corrosion medium, together with the physical barrier of the epoxy and the sheet structure of the graphene. Fu et al. [172] used a hybrid coating consisting of alternating graphene layers and polymer layers for the protection of AA2024-T3, an aluminium alloy. The optimised coating consisted of five layers, with two graphene layers sandwiched between three polymer layers, where the polymer was polyvinyl butyral. Again, the layered structure was shown to enhance the protective properties of the

coating, with diffusion of the corrosion species being significantly limited and inhibited by the two graphene layers. Gao et al. [173] immobilised heparin on GO to give heparinised GO which was then sandwiched between two chitosan layers. This layering was repeated five times to give a multilayer with several isolated graphene layers for the corrosion protection of a magnesium alloy. The chitosan was employed to give good biocompatibility and it was shown that it promoted the adhesion and proliferation of endothelial cells. It was concluded that the layered coating improved not only the biocompatibility of the surface but simultaneously improved the corrosion resistance making this approach suitable for implant materials.

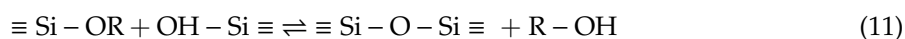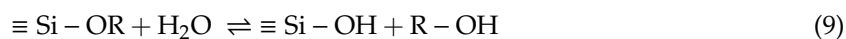## 6. Graphene Modified Zinc Rich Coatings

While zinc rich coatings have been known for a considerable time, there is still significant interest in further developing these systems by adding graphene, rGO or GO to the system [174]. These coatings are interesting because they not only provide barrier protection, but also act as sacrificial coatings, preferentially corroding and protecting the underlying corrosion susceptible metal or alloy. As the standard reduction potential of the $Zn|Zn^{2+}$ couple is -0.76 V, it will form the anode in a galvanic cell when coupled with iron, steel, copper and indeed various light-weight aluminium alloys. Consequently, when a defect occurs in a coating the Zn is dissolved, protecting the substrate, which becomes the cathode in the cell. In addition, the zinc corrosion products, such as $Zn(OH)_2$ and ZnO, have the potential to seal the defects, further enhancing the protective property of the coating. However, these coatings have a limited lifetime and as the metallic zinc content is lowered and the conducting path between the substrate and zinc is lost, the coatings become ineffective. This can be addressed to some extent by increasing the Zn loading, but this approach has been shown to reduce adhesion [175]. In more recent years, graphene has been added to the zinc coatings to increase the electrical conductivity between the metallic zinc particles and the underlying substrates, while the impermeable nature of the graphene flakes, leading to a reduction in ion transport, can be employed to provide additional barrier protection [176,177].

A number of studies have been carried out with graphene-modified zinc-rich epoxy single [160,178–180], layered and multi-layered coatings [181,182] and silicate/Zn/graphene coatings [183]. In all cases it has been shown that the addition of graphene enhances the corrosion protection properties. The barrier protective properties of the zinc-rich epoxy coatings have been enhanced further by using magnetic GO oriented in a magnetic field [184,185]. In this case magnetic iron oxide nanoparticles were coupled with GO and a magnetic field was then employed to give GO nanosheets parallel to the surface. In addition, efficient anti-corrosion coatings have been formulated using electroplated Zn/GO nanocomposite coatings [186] and low-pressure cold-sprayed coatings [187]. For example, Li et al. [188] and Moshgi Asl et al. [189] used pulsed electrodeposition while galvanostatic deposition [190] has also been employed to form Zn/GO composites with high stability and good corrosion protection performance. In a recent study the microstructure and corrosion protection properties of electrodeposited Zn/GO and Zn/GO/Zn multilayers were studied and compared [191]. The added GO was shown to induce a reduction in the size of the Zn grains and decrease the corrosion rate, while cross-sections of the Zn/GO/Zn multilayer coatings showed that the GO reduced the dissolution of the underlying Zn layer by inhibiting the permeation of OH^- and Cl^- ions. Tin and nickel have also been combined with zinc to give SnZn/GO composites [192] and NiZn/GO [193] with very good corrosion protection properties.

7. Graphene Combined with Sol-Gels as Protective Coatings

In the last few decades, sol-gel coatings have been developed as anti-corrosion coatings and have shown good corrosion protection in various high demand applications [10,194]. In the sol-gel process the coating is created through a series of hydrolysis, condensation and polycondensation reactions, with liquid precursors such as silicon alkoxides, as illustrated in Equations (9)–(11) [195]. These reactions are normally carried out at temperatures close to room temperature, while other

substances, such as corrosion inhibitors and pigments, can be easily incorporated to give a simple and very versatile low temperature coating technology. While the dense Si-O-Si network can provide an effective barrier preventing the diffusion of corrosion agents, such as O_2, H_2O and Cl^-, these coatings have a tendency to develop micro pores during the film forming process due to solvent evaporation and therefore various additives have been used, such as corrosion inhibitors [196] to enhance the performance of the coatings.

$$\equiv Si - OR + H_2O \rightleftharpoons \equiv Si - OH + R - OH \tag{9}$$

$$\equiv Si - OH + OH - Si \equiv \rightleftharpoons \equiv Si - O - Si \equiv + H_2O \tag{10}$$

$$\equiv Si - OR + OH - Si \equiv \rightleftharpoons \equiv Si - O - Si \equiv + R - OH \tag{11}$$

More recently, GO has been incorporated into this sol-gel network to give further improvement in the corrosion protection of the coatings [197]. Sol-gels modified with GO [198–201], functionalised GO [202–204] and GO loaded corrosion inhibitors [205,206] have all been employed to enhance the protective properties of the coatings. For example, Parkhizer et al. [202] incorporated silane functionalised GO nanosheets into a silane coating and compared this coating with the non-functionalised GO-based silane coating. It was found that the functionalised GO significantly enhanced the corrosion protection performance of the coating. This was attributed to the very good compatibility of the functionalised GO nanofillers with the silane matrix, reducing porosity. Maeztu et al. [207] formulated a multilayer system where GO was combined with the sol-gel and used as the initial layer, then an outer fluorinated hydrophobic sol-gel layer was applied. This multilayer was shown to provide good corrosion protection to the underlying aluminium alloy substrate. Multilayer graphene-modified sol-gel coatings have also been employed to protect magnesium alloys [208] and in this case a comparative study on the performance of sol-gels modified with carbon nanotubes (CNTs) and COOH-functionalised graphene showed that the graphene-containing sol-gels were superior, inhibiting the transport of Cl^- to the surface of the substrate.

GO embedded in a sol-gel-based silane coating has also been employed to pre-treat a steel substrate to enhance the adhesion of an epoxy top coating [204]. This approach leads to a significant improvement in the corrosion resistance and adhesion properties of the top epoxy coating and this was attributed to higher compatibility between the epoxy and silane matrix and the formation of covalent bonds with the top epoxy coating.

8. Graphene and Layered Double Hydroxides or MOFs

Layered double hydroxides (LDHs), represented as $[M_{1-x}^{2+}M_x^{3+}(OH)_2]^{x+}(A^{n-})_{x/n}mH_2O$ where M^{2+} and M^{3+} are divalent and trivalent cations, respectively, and A^{n-} are anions, have been used in a number of different applications, including environmental [209], electrocatalysts for the oxidation of water [210], supercapacitors [211] and corrosion resistant layers [212]. LDHs have been employed for their corrosion protective properties [213,214] with a considerable interest in exploiting their ion exchange behaviour to release corrosion inhibitors [215,216]. Moreover, the insulating LDH can limit the formation of the graphene-metal galvanic couple, avoiding micro-galvanic corrosion [217]. Nevertheless, LDHs have a microporous structure and therefore provide a pathway for the diffusion of chloride anions and oxygen; however, it has been argued that LDHs can in fact be used as a chloride trap in organic polymeric coatings [218] to give higher and more long term corrosion protection.

Graphene and its derivatives, GO and rGO, have been utilised with LDHs to inhibit inward diffusion as the impermeable graphene nanosheets can impede the transport of ions and molecules to the underlying substrate. For example, Yan et al. [219] deposited an rGO/zinc-aluminium LDH (rGO/Zn-Al LDH) at a magnesium alloy using a simple hydrothermal crystallisation process. It was shown that the rGO nanosheets and LDH layers grew on the magnesium substrate without a particular orientation to give a superior impermeable interface that prevented the corrosion promoting species

from reaching the substrate. Lu et al. [220] developed a continuous flow method to deposit rGO/Zn-Al LDH at an aluminium alloy to give very good corrosion protection properties. Again, the enhanced corrosion resistance was explained in terms of the barrier effect provided by rGO on the diffusion of water, oxygen and chloride anions.

The application of the rGO-modified LDHs as a self-healing coating has also been studied, with both molybdate [221] and aspartate [122] anions incorporated as the anions in the LDH structure and then released in a controlled fashion to protect the underlying corrosion susceptible substrate. In addition, these LDHs have been incorporated within epoxy coatings. Yu et al. [222] incorporated rGO/Zn-Al LDH modified with aminopropyl triethoxysilane into a waterborne epoxy coating as an anti-corrosion agent. Using a ratio of GO:Zn-Al-LDH of 2:1 and a 0.5 wt% ratio within the epoxy coating very good corrosion protection was achieved. Likewise, Zhong et al. [122] employed an inhibitor containing rGO/LDH as a filler within an epoxy coating which showed outstanding self-healing performance.

Metal organic frameworks (MOFs), which consist of metal ions like Zn^{2+} and organic ligands, such as imidazoles, are well known for their porosity. There have been relatively few reports where these have been employed in the formulation of protective coatings. However, there are two recent reports where MOFs have been used with graphene as nanocontainers to encapsulate corrosion inhibitors. For example, GO/MOFs loaded with benzotriazole and embedded within polyvinyl butyral have been utilised to protect copper [223] while they have also been incorporated within epoxy coatings to give protective coatings [224].

9. Nanoparticle Decorated and Metal Oxide Modified Graphene

As detailed earlier the aggregation of GO and rGO sheets, through van der Waals interactions, continues to remain challenging in the development of graphene-based protective coatings, as these aggregation reactions reduce the service life of a coating. Consequently, research has focussed on the surface modification of GO sheets and this has been achieved through chemical functionalisation and the addition of conducting polymers, as described earlier, and by decorating the GO sheets with nanoparticles. It has been shown that nanoparticles, such as gold [225], silver [226], platinum [227], titanium dioxide [228], zinc oxide [229] and iron oxides [230] can be deposited or grafted to the basal planes of GO, where the oxygen functionalities can provide reactive sites for the nucleation and growth of the nanoparticles. As a result, these nanoparticles can act as a spacer layer between the GO sheets minimising aggregation of the sheets. Likewise, this arrangement inhibits the agglomeration of the nanoparticles.

Various nanoparticle-modified GO sheets have been formed and effectively dispersed within epoxy coatings to give more protective coatings. Silicon dioxide, SiO_2, particles also termed silica, are frequently used within coatings [231] and also combined with GO [74,232] and employed in coating formulations. The interest in SiO_2 nanoparticles stems from their excellent chemical and thermal stability, hydrophilicity and low cost. A number of studies have shown that SiO_2-modifed GO epoxy coatings have more protective properties than the corresponding GO/epoxy formulations with the nano-SiO_2 playing an important role in improving the dispersion of GO sheets [233,234]. When GO is modified with SiO_2 it becomes more hydrophilic and while this improves its dispersion within coatings, it can also reduce the protective nature of the coatings. Indeed, it has been shown that the hydrophobic nature of the surface is reduced after the incorporation of GO/SiO_2 [235]. In a recent study this was addressed by functionalising the SiO_2 with hydrophobic alkyl side chains achieving a balance between the hydrophilicity required for dispersing the SiO_2-modified GO sheets and hydrophobicity required to give protective coatings [236].

Different oxides have been coupled with graphene including MgO to enhance the interfacial bonding between graphene and magnesium substrates [237], praseodymium-decorated graphene for the protection of a magnesium AZ31 alloy [238], while silver nanoparticles have been combined with GO to give protective coatings with antibacterial activity [62,239,240]. Additional metals/oxides

such as TiO_2 [241–243], ZnO [244–246], CeO_2 [247] and NiCo [248] have been coupled with graphene to enhance dispersion and corrosion protection. Moreover, antimony tin oxide powder has been mixed with graphene sheets and added to epoxy coatings to give protective coatings with conducting properties [249].

Semiconducting oxides have also been employed as radical scavengers and UV shields to reduce weathering that occurs with polymeric systems when exposed to sunlight. This photo-degradation can be significantly reduced by using oxides that can absorb or scatter the light. For example, CeO_2 is a good UV blocker and it has been combined with GO to give more stable outdoor coatings [250]. Semiconducting oxides are also attractive for photogenerated cathodic protection, which is attracting interest as a corrosion protection method [251]. This approach is illustrated in the schematic shown in Figure 6. On absorption of light photons electrons are promoted from the valence to the conduction band and if these electrons can be shuttled or transferred to the corrosion susceptible metal or alloy then the system can be polarised to potentials well below the corrosion potential or sufficiently reduced to move the system into the immune region, as illustrated in the Pourbaix diagram, Figure 6. Graphene has been successfully employed to shuttle the electrons from the conduction band to the substrate electrode. For example, graphene and TiO_2 have been employed for enhanced photogenerated cathodic protection combined with $Co(OH)_2$ [252], Ag [253], WO_3 [254] and SnO_2 [255].
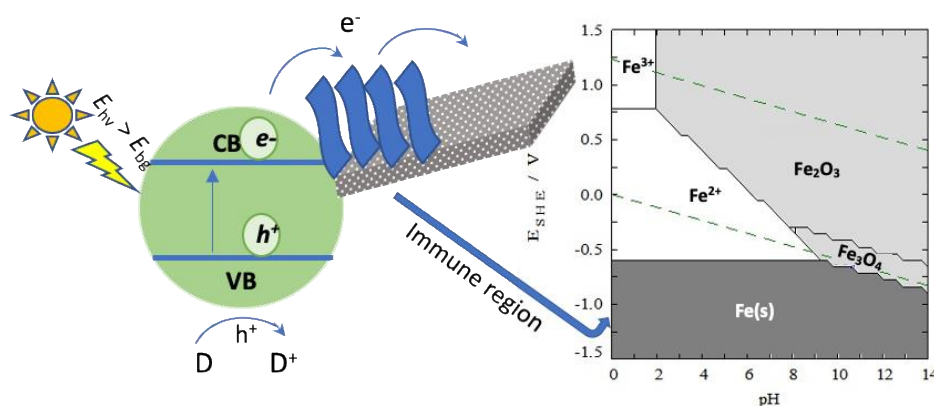

Figure 6. Schematic of photocathodic protection, with graphene sheets shuttling the electrons from the semiconductor conduction band to the metal/alloy.

10. Hexagonal Boron Nitride and Graphitic Carbon Nitride

Two-dimensional hexagonal boron nitride (h-BN), frequently described as "white graphene", has graphene-like sheets consisting of N and B atoms, bound by strong covalent bonds, while the layers are held together by weak van der Waals forces. This 2D material can be formed using chemical vapour deposition [256]; however, the solution-based exfoliation of bulk BN powders is more commonly employed to give large quantities of the layered sheet structures. While bulk boron nitride is insulating, bipolar electrochemical techniques can be employed to give electrochemical exfoliation [257]. These h-BN layers are hydrophobic, chemically stable and non-conducting and therefore will not generate local galvanic corrosion cells with the corrosion susceptible substrate, while their impermeable nature will inhibit the inward penetration of corrosion promoting ions, such as Cl^- and O_2. Indeed, it was shown that h-BN coatings can impede the transport of oxygen, inhibiting corrosion [258] while Galbiati et al. [259], in comparing the oxidation of copper coated by graphene and h-BN single layers, found that while graphene had better short term corrosion protection properties, the h-BN, due to its insulating nature and inability to form a galvanic couple with copper, provided superior long term corrosion protection. This makes h-BN an attractive 2D material for the formulation of corrosion protective coatings and films [260,261]. Nanosheets of h-BN have been employed to protect copper foil exposed to high temperatures of 250 °C in air [262], while h-BN nanosheets have been grown on silver substrates using chemical vapour deposition and shown to protect the silver

from chemical attack [263]. Boron inks have also been used to form BN coatings at copper with highly impermeable coatings with good anti-corrosion properties [264].

Recently, h-BN/polymer hybrid coatings have been utilised in corrosion protection. As with graphene, homogenous dispersions of h-BN nanosheets in the polymer matrix is crucial in forming protective coatings. In a recent study, h-BN was dispersed in an epoxy matrix using a carboxylated aniline trimer which acted as a dispersant by forming strong π–π interactions with the h-BN nanosheets to give protective anticorrosion coatings [265]. Likewise, poly(2-butyl aniline) [266] and polyethylenimine [267] can be employed as an effective dispersing agent for h-BN in epoxy coatings. Several h-BN modified epoxy coatings have been formulated and used to protect corrosion susceptible electrodes and these have been successfully formed using functionalised h-BN [268–270], h-BN modified by Fe_3O_4 nanoparticles [271] and Al_2O_3 nanoparticles [272], and h-BN with added corrosion inhibitors [273]. Other polymer coatings have also been considered. For example, Husain et al. [274] dispersed h-BN in a polyvinyl alcohol (PVA) coating to protect SS316 stainless steel from corrosion. The low corrosion current density of 5.14×10^{-8} A cm^{-2} was attributed to the inert and dielectric nature of h-BN. Nanosheets of h-BN have also been successfully employed as nanofillers in polyvinyl butyral coatings [275], resulting in highly impermeable polymeric composites for corrosion protection.

Another interesting 2D material is graphitic carbon nitride (g-C_3N_4). Carbon nitrides are layered π-conjugated polymeric materials, with planes comparable to graphite and consisting of C and N with linear tri-s-triazine networks. These bulk materials are synthesised from melamine, urea or cyanamide using a thermal process [276] and then the nanosheets can be formed using etching or liquid exfoliation. These sheets, like graphene, have high surface area with good interfacial charge transfer properties. Similar to h-BN, g-C_3N_4 nanosheets are a very good substitute for graphene providing good barriers for the penetration of corrosive ions. Using chemical vapour deposition, g-C_3N_4 nanosheets were formed on a magnesium alloy to give significantly improved corrosion resistance [277]. Likewise, g-C_3N_4 nanosheets have been employed as a nanofiller in epoxy coatings, with g-C_3N_4/ZnO nanocomposites being utilised as a nanofiller in enhancing the corrosion resistant performance of epoxy coatings [278]. In other studies, a polystyrene/g-C_3N_4 anti-corrosion coating formulation was used to give highly protective coatings for copper [279], while PANi/g-C_3N_4 composites have been employed to protect iron [280] and electroactive polyimide/g-C_3N_4 composites were utilised to protect 316L SS, carbon steel and an aluminium alloy [281]. In addition, a g-C_3N_4/MoOx nanocomposite was used as a nanofiller in epoxy coatings to enhance the anti-corrosion performance of an AA2024 Al alloy [282].

In addition, g-C_3N_4, is also attracting considerable interest as a photocatalyst [283,284]. Moreover, the electron-hole pair can be generated using visible light, while the positions of the conductance, valence bands and bandgap energy can be varied by doping or copolymerisation [276]. Consequently, g-C_3N_4 has been employed in the photocathodic protection of 316 stainless steel and Q235 carbon steel [285]. Clearly, both h-BN and g-C_3N_4 have a bright future in corrosion protection.

11. Conclusions and Future Outlook

It is clear from the reports reviewed and the growing number of publications, where graphene is employed in corrosion protection, that graphene and its derivatives, GO and rGO, are interesting candidates in the formulation of corrosion protective films and coatings. As detailed earlier, graphene, rGO and GO can be coupled with a number of other materials to give protective composite coatings and these combinations include various organic coatings, such as epoxy and polyurethane, and zinc rich, sol-gel, LDH, MOF and conducting polymers. While it is difficult to functionalise rGO due to the lack of groups that can be activated, GO, with its oxygen containing groups, is easily functionalised with various chemical groups or grafted to a polymer, enabling its better integration into polymer composites, while metal nanoparticles, conducting oligomers or polymers and surfactants can be employed as intercalators in an attempt to reduce aggregation of the 2D nanosheets.

Nevertheless, the application of graphene as a corrosion protection layer remains somewhat controversial. There is a general consensus that single or multiple layers of conducting graphene or rGO

at metal or alloy surfaces is complicated by galvanic coupling with the metal substrate, which can give rise to higher rates of corrosion in the long term. While the layered rGO has very good impermeable properties inhibiting the diffusion of corrosion promoting ions, such as O_2, H_2O and especially Cl^-, galvanic corrosion will occur at defect sites. More success has been achieved by combining GO, functionalised GO or metal nanoparticle decorated GO with polymers to give composite or hybrid coatings and by coupling rGO with zinc-rich coatings, where the good conductivity of the reduced graphene can be exploited to enhance the anti-corrosion properties of the sacrificial zinc-based coatings.

This research field is still in its infancy and a number of challenges exist and must be addressed before graphene-based composites can be employed in corrosion protection. Long-term corrosion is required in all real applications and one of the biggest challenges is the prevention of graphene sheet aggregation over an extended time frame. This has been partially addressed by functionalised GO and by incorporating other intercalating agents, but more long term corrosion studies are required to establish if these approaches can be utilised to give long-term corrosion protective coatings. Moreover, while a lot of research has focussed on solvent-based organic coating formulations, waterborne resins and coatings are more environmentally acceptable, but the good dispersion of rGO and functionalised GO is considerably more difficult in these aqueous-based systems. It is well established that protective coatings require very good long-term dispersion of graphene and further efforts are needed to develop new dispersion strategies for rGO and functionalised GO in aqueous solutions. In addition, the development of a cost-effective and large-scale synthesis that can be employed in the scale-up of not only graphene but other impermeable 2D materials is required before these materials can be exploited in the formulation of corrosion protection coatings. There are added concerns over the environmental impact of graphene. As GO contains polar oxygen-containing groups, it is reasonably soluble in water and GO nanosheets can enter the aquatic system and have adverse effects on the aquatic ecosystem. Therefore, GO-modified coatings must be stable and not prone to leaching of GO flakes at corrosion sites. Consequently, studies that monitor the leaching of GO during the deterioration and delamination of coatings are essential from an environmental perspective.

Nonetheless, with the further development of graphene-based coatings accompanied by a better understanding of the precise role of graphene in the corrosion protection mechanism, these materials have a promising future as additives in corrosion protective coatings. The emergence of graphene-like 2D materials, such as h-BN, is also interesting as h-BN has similar impermeable behaviour as graphene but is insulating, minimising the establishment of galvanic couples with the metal or alloy being protected. Indeed, there may be advantages in using both h-BN and GO in coating formulations. Likewise, g-C_3N_4 is especially interesting in terms of its band structure, with the generation of electron and hole pairs using visible light. Consequently, g-C_3N_3 or g-C_3N_3 coupled with rGO or GO may have applications in the photocathodic protection of metals and alloys.

Author Contributions: Conceptualization, writing initial draft and editing, C.B.B.; writing, review and editing T.Y., B.H. and D.d.S.A. All authors have read and agreed to the published version of the manuscript.

Conflicts of Interest: The authors declare no conflict of interest.

References

1. Usman, B.J.; Scenini, F.; Curioni, M. Corrosion Testing of Anodized Aerospace Alloys: Comparison between Immersion and Salt Spray Testing using Electrochemical Impedance Spectroscopy. *J. Electrochem. Soc.* **2020**, *167*, 041505. [CrossRef]
2. Rathish, R.J.; Prabha, S.S.; Dorothy, R.; Jancyrani, S.; Rajendran, S.; Singh, G.; Kumaran, S.S. Corrosion issues in electronic equipments—An overview. *Int. J. Corros. Scale Inhib.* **2019**, *8*, 799–815. [CrossRef]
3. Li, J.; Luo, X.; Ma, G.; Wang, J.; Pan, J.; Ruan, Q. The effect of cold rolled reduction ratios on grain boundary character and mechanical properties of the SUS301L austenitic stainless steel. *Mater. Res. Express* **2019**, *6*, 126587. [CrossRef]

4.   Wang, K.; Wang, Z.M.; Song, G.-L. Batch transportation of oil and water for reducing pipeline corrosion. *J. Pet. Sci. Eng.* **2020**, *195*, 107583. [CrossRef]

5.   Saito, N.; Tsuchiya, Y.; Akai, Y.; Omura, H.; Takada, T.; Hara, N. Corrosion performance of metals for supercritical water, oxidation-utilized organic waste-processing reactors. *Corrosion* **2006**, *62*, 383–394. [CrossRef]

6.   Deshwal, G.K.; Panjagari, N.R. Review on metal packaging: Materials, forms, food applications, safety and recyclability. *J. Food Sci. Technol.* **2020**, *57*, 2377–2392. [CrossRef]

7.   Sumant, A.V.; Krauss, A.R.; Gruen, D.M.; Auciello, O.; Erdemir, A.; Williams, M.; Artiles, A.F.; Adams, W. Ultrananocrystalline diamond film as a wear-resistant and protective coating for mechanical seal applications. *Tribol. Trans.* **2005**, *48*, 24–31. [CrossRef]

8.   Tan, L.; Ren, X.; Sridharan, K.; Allen, T.R. Corrosion behavior of Ni-base alloys for advanced high temperature water-cooled nuclear plants. *Corros. Sci.* **2008**, *50*, 3056–3062. [CrossRef]

9.   Qu, D.R.; Zheng, Y.G.; Jing, H.M.; Yao, Z.M.; Ke, W. High temperature naphthenic acid corrosion and sulphidic corrosion of Q235 and 5Cr1/2Mo steels in synthetic refining media. *Corros. Sci.* **2006**, *48*, 1960–1985. [CrossRef]

10.   Becker, M. Chromate-free chemical conversion coatings for aluminum alloys. *Corros. Rev.* **2019**, *37*, 321–342. [CrossRef]

11.   Szklarska-Smialowska, Z. Pitting corrosion of aluminum. *Corros. Sci.* **1999**, *41*, 1743–1767. [CrossRef]

12.   Walsh, F.C.; Wang, S.; Zhou, N. The electrodeposition of composite coatings: Diversity, applications and challenges. *Curr. Opin. Electrochem.* **2020**, *20*, 8–19. [CrossRef]

13.   Carragher, U.; Branagan, D.; Breslin, C.B. The influence of carbon nanotubes on the protective properties of polypyrrole formed at copper. *Materials* **2019**, *12*, 2587. [CrossRef] [PubMed]

14.   Mao, S.; Li, W.; Zeng, X.; Yi, A.; Liao, Z.; Zhu, W. Multiple transitional metal oxides conversion coating on AA6063 toward corrosion protection and electrical conductivity. *Surf. Coat. Technol.* **2020**, *397*, 125819. [CrossRef]

15.   El Abedin, S.Z.; Welz-Biermann, U.; Endres, F. A study on the electrodeposition of tantalum on NiTi alloy in an ionic liquid and corrosion behaviour of the coated alloy. *Electrochem. Commun.* **2005**, *7*, 941–946. [CrossRef]

16.   Yang, Y.; Liu, S.; Chi, C.; Hao, J.; Zhao, J.; Xu, Y.; Li, Y. Electrodeposition of a continuous, dendrite-free aluminum film from an ionic liquid and its electrochemical properties. *J. Mater. Sci. Mater. Electron.* **2020**, *31*, 9937–9945. [CrossRef]

17.   Guo, S.; Dong, S. Graphene nanosheet: Synthesis, molecular engineering, thin film, hybrids and energy and analytical applications. *Chem. Soc. Rev.* **2011**, *40*, 2644–2672. [CrossRef]

18.   Lee, C.W.; Suh, J.M.; Jang, H.W. Chemical Sensors Based on Two-Dimensional (2D) Materials for Selective Detection of Ions and Molecules in Liquid. *Front. Chem.* **2019**, *7*, 708. [CrossRef]

19.   Nag, A.; Mitra, A.; Mukhopadhyay, S.C. Graphene and its sensor-based applications: A review. *Sens. Actuators A Phys.* **2018**, *270*, 177–194. [CrossRef]

20.   Chang, Y.-M.; Lin, H.-W.; Li, L.-J.; Chen, H.-Y. Two-dimensional materials as anodes for sodium-ion batteries. *Mater. Today Adv.* **2020**, *6*, 100054. [CrossRef]

21.   Divyapriya, G.; Nidheesh, P.V. Importance of Graphene in the Electro-Fenton Process. *ACS Omega* **2020**, *5*, 4725–4732. [CrossRef] [PubMed]

22.   Yu, T.; Breslin, C.B. Graphene-modified composites and electrodes and their potential applications in the electro-fenton process. *Materials* **2020**, *13*, 2254. [CrossRef] [PubMed]

23.   Li, D.; Lai, W.-Y.; Zhang, Y.-Z.; Huang, W. Printable Transparent Conductive Films for Flexible Electronics. *Adv. Mater.* **2018**, *30*, 1704738. [CrossRef] [PubMed]

24.   Luo, Y.; Que, W.; Yang, C.; Tian, Y.; Yang, Y.; Yin, X. Nitrogen-doped graphene/multiphase nickel sulfides obtained by Ni-C$_3$N$_3$S$_3$ (metallopolymer) assisted synthesis for high-performance hybrid supercapacitors. *Electrochim. Acta* **2019**, *301*, 332–341. [CrossRef]

25.   Geng, P.; Zheng, S.; Tang, H.; Zhu, R.; Zhang, L.; Cao, S.; Xue, H.; Pang, H. Transition metal sulfides based on graphene for electrochemical energy storage. *Adv. Energy Mater.* **2018**, *8*, 1703259. [CrossRef]

26.   Dreyer, D.R.; Park, S.; Bielawski, C.W.; Ruoff, R.S. The chemistry of graphene oxide. *Chem. Soc. Rev.* **2010**, *39*, 228–240. [CrossRef]

27.   Hummers, W.S.; Offeman, R.E. Preparation of graphitic oxide. *J. Am. Chem. Soc.* **1958**, *80*, 1339. [CrossRef]

28. Eda, G.; Chhowalla, M. Chemically derived graphene oxide: Towards large-area thin-film electronics and optoelectronics. *Adv. Mater.* **2010**, *22*, 2392–2415. [CrossRef]

29. Zhang, J.; Yang, H.; Shen, G.; Cheng, P.; Zhang, J.; Guo, S. Reduction of graphene oxide vial-ascorbic acid. *Chem. Commun.* **2010**, *46*, 1112–1114. [CrossRef]

30. Wang, Z.; Zhou, X.; Zhang, J.; Boey, F.; Zhang, H. Direct electrochemical reduction of single-layer graphene oxide and subsequent functionalization with glucose oxidase. *J. Phys. Chem. C* **2009**, *113*, 14071–14075. [CrossRef]

31. Guo, H.-L.; Wang, X.-F.; Qian, Q.-Y.; Wang, F.-B.; Xia, X.-H. A green approach to the synthesis of graphene nanosheets. *ACS Nano* **2009**, *3*, 2653–2659. [CrossRef] [PubMed]

32. Shao, Y.; Wang, J.; Engelhard, M.; Wang, C.; Lin, Y. Facile and controllable electrochemical reduction of graphene oxide and its applications. *J. Mater. Chem.* **2010**, *20*, 743–748. [CrossRef]

33. Nine, M.J.; Cole, M.A.; Tran, D.N.H.; Losic, D. Graphene: A multipurpose material for protective coatings. *J. Mater. Chem. A.* **2015**, *3*, 12580–12602. [CrossRef]

34. Ding, R.; Li, W.; Wang, X.; Gui, T.; Li, B.; Han, P.; Tian, H.; Liu, A.; Wang, X.; Liu, X.; et al. A brief review of corrosion protective films and coatings based on graphene and graphene oxide. *J. Alloys Compd.* **2018**, *764*, 1039–1055. [CrossRef]

35. Othman, N.H.; Ismail, M.C.; Mustapha, M.; Sallih, N.; Kee, K.E.; Jaal, R.A. Graphene-based polymer nanocomposites as barrier coatings for corrosion protection. *Prog. Org. Coat.* **2019**, *135*, 82–99. [CrossRef]

36. Ding, R.; Chen, S.; Lv, J.; Zhang, W.; Zhao, X.-D.; Liu, J.; Wang, X.; Gui, T.-J.; Li, B.-J.; Tang, Y.-Z.; et al. Study on graphene modified organic anti-corrosion coatings: A comprehensive review. *J. Alloys Compd.* **2019**, *806*, 611–635. [CrossRef]

37. Cui, G.; Bi, Z.; Zhang, R.; Liu, J.; Yu, X.; Li, Z. A comprehensive review on graphene-based anti-corrosive coatings. *Chem. Eng. J.* **2019**, *373*, 104–121. [CrossRef]

38. Hussain, A.K.; Al Naib, U.M.B. Recent developments in graphene based metal matrix composite coatings for corrosion protection application: A review. *J. Met. Mater. Miner.* **2019**, *29*, 1–9. [CrossRef]

39. Akhtar, S.; Laoui, T.; Ibrahim, A.; Kumar, A.M.; Ahmed, J.; Toor, I.-U.-H. Few-layers graphene film and copper surface morphology for improved corrosion protection of copper. *J. Mater. Eng. Perform.* **2019**, *28*, 5541–5550. [CrossRef]

40. Yang, S.; Zhuo, K.; Sun, D.; Wang, X.; Wang, J. Preparation of graphene by exfoliating graphite in aqueous fulvic acid solution and its application in corrosion protection of aluminum. *J. Colloid Interface Sci.* **2019**, *543*, 263–272. [CrossRef]

41. Mayavan, S.; Siva, T.; Sathiyanarayanan, S. Graphene ink as a corrosion inhibiting blanket for iron in an aggressive chloride environment. *RSC Adv.* **2013**, *3*, 24868–24871. [CrossRef]

42. Singhbabu, Y.N.; Sivakumar, B.; Singh, J.K.; Bapari, H.; Pramanick, A.K.; Sahu, R.K. Efficient anti-corrosive coating of cold-rolled steel in a seawater environment using an oil-based graphene oxide ink. *Nanoscale* **2015**, *7*, 8035–8047. [CrossRef]

43. Qiang, R.; Hou, K.; Wang, J.; Yang, S. Smooth and dense graphene quantum dots-based lubricating coatings prepared by electrophoretic deposition. *Appl. Surf. Sci.* **2020**, *509*, 145338. [CrossRef]

44. Chavez-Valdez, A.; Shaffer, M.S.P.; Boccaccini, A.R. Applications of graphene electrophoretic deposition. A review. *J. Phys. Chem. B.* **2013**, *117*, 1502–1515. [CrossRef] [PubMed]

45. Singh, B.P.; Nayak, S.; Nanda, K.K.; Jena, B.K.; Bhattacharjee, S.; Besra, L. The production of a corrosion resistant graphene reinforced composite coating on copper by electrophoretic deposition. *Carbon* **2013**, *61*, 47–56. [CrossRef]

46. Ma, Y.; Han, J.; Wang, M.; Chen, X.; Jia, S. Electrophoretic deposition of graphene-based materials: A review of materials and their applications. *J. Mater.* **2018**, *4*, 108–120. [CrossRef]

47. Quezada-Rentería, J.A.; Cházaro-Ruiz, L.F.; Rangel-Mendez, J.R. Synthesis of reduced graphene oxide (rGO) films onto carbon steel by cathodic electrophoretic deposition: Anticorrosive coating. *Carbon* **2017**, *122*, 266–275. [CrossRef]

48. Hwang, M.-J.; Kim, M.-G.; Kim, S.; Kim, Y.C.; Seo, H.W.; Cho, J.K.; Park, I.-K.; Suhr, J.; Moon, H.; Koo, J.C.; et al. Cathodic electrophoretic deposition (EPD) of phenylenediamine-modified graphene oxide (GO) for anti-corrosion protection of metal surfaces. *Carbon* **2019**, *142*, 68–77. [CrossRef]

49. Kamil, M.P.; Kim, M.J.; Ko, Y.G. Direct electro-co-deposition of Ni-reduced graphene oxide composite coating for anti-corrosion application. *Mater. Lett.* **2020**, *273*, 127911. [CrossRef]

50. Boukhvalov, D.W.; Bazylewski, P.F.; Kukharenko, A.I.; Zhidkov, I.S.; Ponosov, Y.S.; Kurmaev, E.Z.; Cholakh, S.O.; Lee, Y.H.; Chang, G.S. Atomic and electronic structure of a copper/graphene interface as prepared and 1.5 years after. *Appl. Surf. Sci.* **2017**, *426*, 1167–1172. [CrossRef]

51. Xu, X.; Yi, D.; Wang, Z.; Yu, J.; Zhang, Z.; Qiao, R.; Sun, Z.; Hu, Z.; Gao, P.; Peng, H.; et al. Greatly enhanced anticorrosion of Cu by commensurate graphene coating. *Adv. Mater.* **2018**, *30*, 1702944. [CrossRef] [PubMed]

52. Scardamaglia, M.; Struzzi, C.; Zakharov, A.; Reckinger, N.; Zeller, P.; Amati, M.; Gregoratti, L. Highlighting the dynamics of graphene protection toward the oxidation of copper under operando conditions. *ACS Appl. Mater. Interfaces* **2019**, *11*, 29448–29457. [CrossRef]

53. Álvarez-Fraga, L.; Rubio-Zuazo, J.; Jiménez-Villacorta, F.; Climent-Pascual, E.; Ramírez-Jiménez, R.; Prieto, C.; de Andrés, A. Oxidation mechanisms of copper under graphene: The role of oxygen encapsulation. *Chem. Mater.* **2017**, *29*, 3257–3264. [CrossRef]

54. Schriver, M.; Regan, W.; Gannett, W.J.; Zaniewski, A.M.; Crommie, M.F.; Zettl, A. Graphene as a long-term metal oxidation barrier: Worse than nothing. *ACS Nano* **2013**, *7*, 5763–5768. [CrossRef] [PubMed]

55. Bellucci, F. Galvanic corrosion between nonmetallic composites and metals. I. Effect of metal and of temperature. *Corrosion* **1991**, *47*, 808–819. [CrossRef]

56. Naghdi, S.; Jaleh, B.; Ehsani, A. Electrophoretic deposition of graphene oxide on aluminum: Characterization, low thermal annealing, surface and anticorrosive properties. *Bull. Chem. Soc. Jpn.* **2015**, *88*, 722–728. [CrossRef]

57. Jang, H.; Kim, J.-H.; Kang, H.; Bae, D.; Chang, H.; Choi, H. Reduced graphene oxide as a protection layer for Al. *Appl. Surf. Sci.* **2017**, *407*, 1–7. [CrossRef]

58. Hares, E.; El-Shazly, A.H.; El-Kady, M.F.; Hammad, A.S. Electrophoretic deposition of graphene oxide nanosheets on copper pipe for corrosion protection. *Arab. J. Sci. Eng.* **2019**, *44*, 5559–5569. [CrossRef]

59. Ho, C.-Y.; Huang, S.-M.; Lee, S.-T.; Chang, Y.-J. Evaluation of synthesized graphene oxide as corrosion protection film coating on steel substrate by electrophoretic deposition. *Appl. Surf. Sci.* **2019**, *477*, 226–231. [CrossRef]

60. Ryu, S.; Kwon, Y.J.; Kim, Y.; Lee, J.U. Corrosion protection coating of three-dimensional metal structure by electrophoretic deposition of graphene oxide. *Mater. Chem. Phys.* **2020**, *250*, 123039. [CrossRef]

61. Jena, G.; Vanithakumari, S.C.; Polaki, S.R.; George, R.P.; Philip, J.; Amarendra, G. Electrophoretically deposited graphene oxide–polymer bilayer coating on Cu-Ni alloy with enhanced corrosion resistance in simulated chloride environment. *J. Coat. Technol. Res.* **2019**, *16*, 1317–1335. [CrossRef]

62. Jena, G.; Anandkumar, B.; Vanithakumari, S.C.; George, R.P.; Philip, J.; Amarendra, G. Graphene oxide-chitosan-silver composite coating on Cu-Ni alloy with enhanced anticorrosive and antibacterial properties suitable for marine applications. *Prog. Org. Coat.* **2020**, *139*, 105444. [CrossRef]

63. Srimaneepong, V.; Rokaya, D.; Thunyakitpisal, P.; Qin, J.; Saengkiettiyut, K. Corrosion resistance of graphene oxide/silver coatings on Ni–Ti alloy and expression of IL-6 and IL-8 in human oral fibroblasts. *Sci. Rep.* **2020**, *10*, 3247. [CrossRef]

64. Asgar, H.; Deen, K.M.; Rahman, Z.U.; Shah, U.H.; Raza, M.A.; Haider, W. Functionalized graphene oxide coating on Ti6Al4V alloy for improved biocompatibility and corrosion resistance. *Mater. Sci. Eng. C* **2019**, *94*, 920–928. [CrossRef]

65. Senthilvasan, P.A.; Rangarajan, M. Corrosion protection of mild steel by graphene-based films. *Mater. Res. Express* **2018**, *5*, 085020. [CrossRef]

66. Xu, H.; Zang, J.; Yuan, Y.; Tian, P.; Wang, Y. In situ preparation of graphene coating bonded to stainless steel substrate via Cr–C bonding for excellent anticorrosion and wear resistant. *Appl. Surf. Sci.* **2019**, *492*, 199–208. [CrossRef]

67. Pinto, D.; Bernardo, L.; Amaro, A.; Lopes, S. Mechanical properties of epoxy nanocomposites using titanium dioxide as reinforcement—A review. *Constr. Build. Mater.* **2015**, *95*, 506–524. [CrossRef]

68. Oliveira, J.D.; Rocha, R.C.; Galdino, A.G.D.S. Effect of Al_2O_3 particles on the adhesion, wear, and corrosion performance of epoxy coatings for protection of umbilical cables accessories for subsea oil and gas production systems. *J. Mater. Res. Technol.* **2019**, *8*, 1729–1736. [CrossRef]

69. Ruhi, G.; Bhandari, H.; Dhawan, S.K. Designing of corrosion resistant epoxy coatings embedded with polypyrrole/SiO_2 composite. *Prog. Org. Coat.* **2014**, *77*, 1484–1498. [CrossRef]

70. Behzadnasab, M.; Mirabedini, S.M.; Esfandeh, M. Corrosion protection of steel by epoxy nanocomposite coatings containing various combinations of clay and nanoparticulate zirconia. *Corros. Sci.* **2013**, *75*, 134–141. [CrossRef]

71. Wan, C.; Chen, B. Reinforcement and interphase of polymer/graphene oxide nanocomposites. *J. Mater. Chem.* **2012**, *22*, 3637–3646. [CrossRef]

72. Li, Z.; Li, J.; Cui, J.; Qiu, H.; Yang, G.; Zheng, S.; Yang, J. Dispersion and parallel assembly of sulfonated graphene in waterborne epoxy anticorrosion coatings. *J. Mater. Chem. A* **2019**, *7*, 17937–17946. [CrossRef]

73. Xie, Y.; Liu, C.; Liu, W.; Liang, L.; Wang, S.; Zhang, F.; Shi, H.; Yang, M. A novel approach to fabricate polyacrylate modified graphene oxide for improving the corrosion resistance of epoxy coatings. *Colloids Surf. A Physicochem. Eng. Asp.* **2020**, *593*, 124627. [CrossRef]

74. Ramezanzadeh, B.; Haeri, Z.; Ramezanzadeh, M. A facile route of making silica nanoparticles-covered graphene oxide nanohybrids (SiO$_2$-GO); fabrication of SiO$_2$-GO/epoxy composite coating with superior barrier and corrosion protection performance. *Chem. Eng. J.* **2016**, *303*, 511–528. [CrossRef]

75. Yu, Z.; Di, H.; Ma, Y.; Lv, L.; Pan, Y.; Zhang, C.; He, Y. Fabrication of graphene oxide-alumina hybrids to reinforce the anti-corrosion performance of composite epoxy coatings. *Appl. Surf. Sci.* **2015**, *351*, 986–996. [CrossRef]

76. Ji, W.F.; Chen, K.Y.; Ke, C.J.; Liao, Y.J.; Liu, W.J.; Tsai, M.H.; Yeh, J.M. Comparative corrosion protection studies of electroactive/non-electroactive epoxy thermoset composites containing conductive rGO/non-conductive GO platelets. *Express Polym. Lett.* **2019**, *13*, 604–617. [CrossRef]

77. Dutta, D.; Ganda, A.N.F.; Chih, J.-K.; Huang, C.-C.; Tseng, C.-J.; Su, C.-Y. Revisiting graphene-polymer nanocomposite for enhancing anticorrosion performance: A new insight into interface chemistry and diffusion model. *Nanoscale* **2018**, *10*, 12612–12624. [CrossRef]

78. Um, J.G.; Jun, Y.-S.; Elkamel, A.; Yu, A. Engineering investigation for the size effect of graphene oxide derived from graphene nanoplatelets in polyurethane composites. *Can. J. Chem. Eng.* **2020**, *98*, 1084–1096. [CrossRef]

79. Jiang, F.; Zhao, W.; Wu, Y.; Dong, J.; Zhou, K.; Lu, G.; Pu, J. Anti-corrosion behaviors of epoxy composite coatings enhanced via graphene oxide with different aspect ratios. *Prog. Org. Coat.* **2019**, *127*, 70–79. [CrossRef]

80. Adeel, M.; Bilal, M.; Rasheed, T.; Sharma, A.; Iqbal, H.M.N. Graphene and graphene oxide: Functionalization and nano-bio-catalytic system for enzyme immobilization and biotechnological perspective. *Int. J. Biol. Macromol.* **2018**, *120*, 1430–1440. [CrossRef]

81. Niyogi, S.; Bekyarova, E.; Itkis, M.E.; McWilliams, J.L.; Hamon, M.A.; Haddon, R.C. Solution properties of graphite and graphene. *J. Am. Chem. Soc.* **2006**, *128*, 7720–7721. [CrossRef]

82. Zhang, Z.; Zhang, W.; Li, D.; Sun, Y.; Wang, Z.; Hou, C.; Chen, L.; Cao, Y.; Liu, Y. Mechanical and anticorrosive properties of graphene/epoxy resin composites coating prepared by in-situ method. *Int. J. Mol. Sci.* **2015**, *16*, 2239–2251. [CrossRef] [PubMed]

83. Sari, M.G.; Ramezanzadeh, B. Epoxy composite coating corrosion protection properties reinforcement through the addition of hydroxyl-terminated hyperbranched polyamide non-covalently assembled graphene oxide platforms. *Constr. Build. Mater.* **2020**, *234*, 117421. [CrossRef]

84. Cui, M.; Ren, S.; Pu, J.; Wang, Y.; Zhao, H.; Wang, L. Poly(o-phenylenediamine) modified graphene toward the reinforcement in corrosion protection of epoxy coatings. *Corros. Sci.* **2019**, *159*, 108131. [CrossRef]

85. Calovi, M.; Dirè, S.; Ceccato, R.; Deflorian, F.; Rossi, S. Corrosion protection properties of functionalised graphene–acrylate coatings produced via cataphoretic deposition. *Prog. Org. Coat.* **2019**, *136*, 105261. [CrossRef]

86. Zhang, C.; Dai, X.; Wang, Y.; Sun, G.; Li, P.; Qu, L.; Sui, Y.; Dou, Y. Preparation and corrosion resistance of ETEO modified graphene oxide/epoxy resin coating. *Coatings* **2019**, *9*, 46. [CrossRef]

87. Chilkoor, G.; Sarder, R.; Islam, J.; ArunKumar, K.E.; Ratnayake, I.; Star, S.; Jasthi, B.K.; Sereda, G.; Koratkar, N.; Meyyappan, M.; et al. Maleic anhydride-functionalized graphene nanofillers render epoxy coatings highly resistant to corrosion and microbial attack. *Carbon* **2020**, *159*, 586–597. [CrossRef]

88. Tian, Y.; Xie, Y.; Dai, F.; Huang, H.; Zhong, L.; Zhang, X. Ammonium-grafted graphene oxide for enhanced corrosion resistance of waterborne epoxy coatings. *Surf. Coat. Technol.* **2020**, *383*, 125227. [CrossRef]

89. Feng, C.; Zhu, L.; Cao, Y.; Di, Y.; Yu, Z.; Gao, G. Performance of coating based on β-CD-g-GO/epoxy composites for the corrosion protection of steel. *Int. J. Electrochem. Sci.* **2019**, *14*, 1855–1868. [CrossRef]

90. Zhou, X.; Huang, H.; Zhu, R.; Chen, R.; Sheng, X.; Xie, D.; Mei, Y. Green modification of graphene oxide with phytic acid and its application in anticorrosive water-borne epoxy coatings. *Prog. Org. Coat.* **2020**, *143*, 105601. [CrossRef]

91. Ramezanzadeh, B.; Niroumandrad, S.; Ahmadi, A.; Mahdavian, M.; Mohamadzadeh Moghadam, M.H. Enhancement of barrier and corrosion protection performance of an epoxy coating through wet transfer of amino functionalized graphene oxide. *Corros. Sci.* **2016**, *103*, 283–304. [CrossRef]

92. Wang, S.; Hu, Z.; Shi, J.; Chen, G.; Zhang, Q.; Weng, Z.; Wu, K.; Lu, M. Green synthesis of graphene with the assistance of modified lignin and its application in anticorrosive waterborne epoxy coatings. *Appl. Surf. Sci.* **2019**, *484*, 759–770. [CrossRef]

93. Rajitha, K.; Mohana, K.N.S.; Mohanan, A.; Madhusudhana, A.M. Evaluation of anti-corrosion performance of modified gelatin-graphene oxide nanocomposite dispersed in epoxy coating on mild steel in saline media. *Colloids Surf. A Physicochem. Eng. Asp.* **2020**, *587*, 124341. [CrossRef]

94. Rajitha, K.; Mohana, K.N.S. Synthesis of graphene oxide-based nanofillers and their influence on the anticorrosion performance of epoxy coating in saline medium. *Diam. Relat. Mater.* **2020**, *108*, 107974. [CrossRef]

95. Parhizkar, N.; Shahrabi, T.; Ramezanzadeh, B. A new approach for enhancement of the corrosion protection properties and interfacial adhesion bonds between the epoxy coating and steel substrate through surface treatment by covalently modified amino functionalized graphene oxide film. *Corros. Sci.* **2017**, *123*, 55–75. [CrossRef]

96. Pourhashem, S.; Rashidi, A.; Vaezi, M.R.; Bagherzadeh, M.R. Excellent corrosion protection performance of epoxy composite coatings filled with amino-silane functionalized graphene oxide. *Surf. Coat. Technol.* **2017**, *317*, 1–9. [CrossRef]

97. Liu, C.; Du, P.; Zhao, H.; Wang, L. Synthesis of l-Histidine-Attached Graphene Nanomaterials and Their Application for Steel Protection. *ACS Appl. Nano Mater.* **2018**, *1*, 1385–1395. [CrossRef]

98. Javidparvar, A.A.; Naderi, R.; Ramezanzadeh, B. L-cysteine reduced/functionalized graphene oxide application as a smart/control release nanocarrier of sustainable cerium ions for epoxy coating anti-corrosion properties improvement. *J. Hazard. Mater.* **2020**, *389*, 122135. [CrossRef]

99. Palaniappan, N.; Cole, I.S.; Kuznetsov, A.E.; Balasubramanian, K.; Justin Thomas, K.R. Experimental and computational studies of a graphene oxide barrier layer covalently functionalized with amino acids on Mg AZ13 alloy in salt medium. *RSC Adv.* **2019**, *9*, 32441–32447. [CrossRef]

100. Ramezanzadeh, M.; Ramezanzadeh, B.; Sari, M.G.; Saeb, M.R. Corrosion resistance of epoxy coating on mild steel through polyamidoamine dendrimer-covalently functionalized graphene oxide nanosheets. *J. Ind. Eng. Chem.* **2020**, *82*, 290–302. [CrossRef]

101. Chen, Y.; Ren, B.; Gao, S.; Cao, R. The sandwich-like structures of polydopamine and 8-hydroxyquinoline coated graphene oxide for excellent corrosion resistance of epoxy coatings. *J. Colloid Interface Sci.* **2020**, *565*, 436–448. [CrossRef]

102. Xiao, Y.-K.; Ji, W.-F.; Chang, K.-S.; Hsu, K.-T.; Yeh, J.-M.; Liu, W.-R. Sandwich-structured rGO/PVDF/PU multilayer coatings for anti-corrosion application. *RSC Adv.* **2017**, *7*, 33829–33836. [CrossRef]

103. Bai, T.; Lv, L.; Du, W.; Fang, W.; Wang, Y. Improving the tribological and anticorrosion performance of waterborne polyurethane coating by the synergistic effect between modified graphene oxide and polytetrafluoroethylene. *Nanomaterials* **2020**, *10*, 137. [CrossRef] [PubMed]

104. Um, J.G.; Habibpour, S.; Jun, Y.-S.; Elkamel, A.; Yu, A. Development of π–π interaction-induced functionalized graphene oxide on mechanical and anticorrosive properties of reinforced polyurethane composites. *Ind. Eng. Chem. Res.* **2020**, *59*, 3617–3628. [CrossRef]

105. Wen, J.-G.; Geng, W.; Geng, H.-Z.; Zhao, H.; Jing, L.-C.; Yuan, X.-T.; Tian, Y.; Wang, T.; Ning, Y.-J.; Wu, L. Improvement of corrosion resistance of waterborne polyurethane coatings by covalent and noncovalent grafted graphene oxide nanosheets. *ACS Omega* **2019**, *4*, 20265–20274. [CrossRef] [PubMed]

106. Zhu, K.; Li, X.; Li, J.; Fei, G.; Wang, J. Synthesis and anticorrosive properties of waterborne isocyanate functionalized graphene/polyurethane nanocomposite emulsion. *J. Funct. Mater.* **2016**, *47*, 06016–06021. [CrossRef]

107. Mo, M.; Zhao, W.; Chen, Z.; Yu, Q.; Zeng, Z.; Wu, X.; Xue, Q. Excellent tribological and anti-corrosion performance of polyurethane composite coatings reinforced with functionalized graphene and graphene oxide nanosheets. *RSC Adv.* **2015**, *5*, 56486–56497. [CrossRef]

108. Wang, H.; He, Y.; Fei, G.; Wang, C.; Shen, Y.; Zhu, K.; Sun, L.; Rang, N.; Guo, D.; Wallace, G.G. Functionalizing graphene with titanate coupling agents as reinforcement for one-component waterborne poly(urethane-acrylate) anticorrosion coatings. *Chem. Eng. J.* **2019**, *359*, 331–343. [CrossRef]

109. Zhao, Z.; Guo, L.; Feng, L.; Lu, H.; Xu, Y.; Wang, J.; Xiang, B.; Zou, X. Polydopamine functionalized graphene oxide nanocomposites reinforced the corrosion protection and adhesion properties of waterborne polyurethane coatings. *Eur. Polym. J.* **2019**, *120*, 109249. [CrossRef]

110. Zhang, F.; Liu, W.; Liang, L.; Wang, S.; Shi, H.; Xie, Y.; Yang, M.; Pi, K. The effect of functional graphene oxide nanoparticles on corrosion resistance of waterborne polyurethane. *Colloids Surf. A Physicochem. Eng. Asp.* **2020**, *591*, 124565. [CrossRef]

111. Rajitha, K.; Mohana, K.N. Application of modified graphene oxide—Polycaprolactone nanocomposite coating for corrosion control of mild steel in saline medium. *Mater. Chem. Phys.* **2020**, *241*, 122050. [CrossRef]

112. Liu, Q.; Ma, R.; Du, A.; Zhang, X.; Yang, H.; Fan, Y.; Zhao, X.; Cao, X. Investigation of the anticorrosion properties of graphene oxide doped thin organic anticorrosion films for hot-dip galvanized steel. *Appl. Surf. Sci.* **2019**, *480*, 646–654. [CrossRef]

113. Rajitha, K.; Mohana, K.N.S.; Nayak, S.R.; Hegde, M.B.; Madhusudhana, A.M. An efficient and eco-friendly anti-corrosive system based on beeswax-graphene oxide nanocomposites on mild steel in saline medium. *Surf. Interfaces* **2020**, *18*, 100393. [CrossRef]

114. Wang, S.; Sun, H.; Ang, H.M.; Tadé, M.O. Adsorptive remediation of environmental pollutants using novel graphene-based nanomaterials. *Chem. Eng. J.* **2013**, *226*, 336–347. [CrossRef]

115. Javidparvar, A.A.; Naderi, R.; Ramezanzadeh, B. Manipulating graphene oxide nanocontainer with benzimidazole and cerium ions: Application in epoxy-based nanocomposite for active corrosion protection. *Corros. Sci.* **2020**, *165*, 108379. [CrossRef]

116. Yu, Z.; Lv, L.; Ma, Y.; Di, H.; He, Y. Covalent modification of graphene oxide by metronidazole for reinforced anti-corrosion properties of epoxy coatings. *RSC Adv.* **2016**, *6*, 18217–18226. [CrossRef]

117. Daradmare, S.; Pradhan, M.; Raja, V.S.; Parida, S. 8-Hydroxyquinoline encapsulated graphene oxide stabilized polystyrene containers based anticorrosion coatings. In Proceedings of the European Corrosion Congress EUROCORR 2017, 20th Internacional Corrosion Congress and the Process Safety Congress 2017, Prague, Czech Republic, 3–7 September 2017.

118. Chen, C.; He, Y.; Xiao, G.; Zhong, F.; Li, H.; Wu, Y.; Chen, J. Synergistic effect of graphene oxide@phosphate-intercalated hydrotalcite for improved anti-corrosion and self-healable protection of waterborne epoxy coating in salt environments. *J. Mater. Chem. C* **2019**, *7*, 2318–2326. [CrossRef]

119. Kasaeian, M.; Ghasemi, E.; Ramezanzadeh, B.; Mahdavian, M.; Bahlakeh, G. Construction of a highly effective self-repair corrosion-resistant epoxy composite through impregnation of 1H-Benzimidazole corrosion inhibitor modified graphene oxide nanosheets (GO-BIM). *Corros. Sci.* **2018**, *145*, 119–134. [CrossRef]

120. Cao, K.; Yu, Z.; Yin, D.; Chen, L.; Jiang, Y.; Zhu, L. Fabrication of BTA-MOF-TEOS-GO nanocomposite to endow coating systems with active inhibition and durable anticorrosion performances. *Prog. Org. Coat.* **2020**, *143*, 105629. [CrossRef]

121. Qian, B.; Ren, J.; Song, Z.; Zhou, Y. One pot graphene-based nanocontainers as effective anticorrosion agents in epoxy-based coatings. *J. Mater. Sci.* **2018**, *53*, 14204–14216. [CrossRef]

122. Zhong, F.; He, Y.; Wang, P.; Chen, C.; Xie, P.; Li, H.; Chen, J. One-step hydrothermal synthesis of reduced graphene oxide/aspartic acid intercalated layered double hydroxide for enhancing barrier and self-healing properties of epoxy coating. *React. Funct. Polym.* **2019**, *145*, 104380. [CrossRef]

123. Asaldoust, S.; Ramezanzadeh, B. Synthesis and characterization of a high-quality nanocontainer based on benzimidazole-zinc phosphate (ZP-BIM) tailored graphene oxides; a facile approach to fabricating a smart self-healing anti-corrosion system. *J. Colloid Interface Sci.* **2020**, *564*, 230–244. [CrossRef] [PubMed]

124. Yu, M.; Zhao, X.; Xiong, L.; Xue, B.; Kong, X.; Liu, J.; Li, S. Improvement of corrosion protection of coating system via inhibitor response order. *Coatings* **2018**, *8*, 365. [CrossRef]

125. Dehghani, A.; Bahlakeh, G.; Ramezanzadeh, B. Synthesis of a non-hazardous/smart anti-corrosion nano-carrier based on beta-cyclodextrin-zinc acetylacetonate inclusion complex decorated graphene oxide (β-CD-ZnA-MGO). *J. Hazard. Mater.* **2020**, *398*, 122962. [CrossRef] [PubMed]

126. Nguyen, T.D.; Nguyen, A.S.; Tran, B.A.; Vu, K.O.; Tran, D.L.; Phan, T.T.; Scharnagl, N.; Zheludkevich, M.L.; To, T.X.H. Molybdate intercalated hydrotalcite/graphene oxide composite as corrosion inhibitor for carbon steel. *Surf. Coat. Technol.* **2020**, *399*, 126165. [CrossRef]

127. Mo, Z.-H.; Luo, Z.; Huang, Q.; Deng, J.-P.; Wu, Y.-X. Superhydrophobic hybrid membranes by grafting arc-like macromolecular bridges on graphene sheets: Synthesis, characterization and properties. *Appl. Surf. Sci.* **2018**, *440*, 359–368. [CrossRef]

128. Li, Y.; Alain-Rizzo, V.; Galmiche, L.; Audebert, P.; Miomandre, F.; Louarn, G.; Bozlar, M.; Pope, M.A.; Dabbs, D.M.; Aksay, I.A. Functionalization of Graphene Oxide by Tetrazine Derivatives: A versatile approach toward covalent bridges between graphene sheets. *Chem. Mater.* **2015**, *27*, 4298–4310. [CrossRef]

129. Gonalves, G.; Marques, P.A.A.P.; Barros-Timmons, A.; Bdkin, I.; Singh, M.K.; Emami, N.; Grácio, J. Graphene oxide modified with PMMA via ATRP as a reinforcement filler. *J. Mater. Chem.* **2010**, *20*, 9927–9934. [CrossRef]

130. Qi, K.; Sun, Y.; Duan, H.; Guo, X. A corrosion-protective coating based on a solution-processable polymer-grafted graphene oxide nanocomposite. *Corros. Sci.* **2015**, *98*, 500–506. [CrossRef]

131. Jiang, F.; Zhao, W.; Wu, Y.; Wu, Y.; Liu, G.; Dong, J.; Zhou, K. A polyethyleneimine-grafted graphene oxide hybrid nanomaterial: Synthesis and anti-corrosion applications. *Appl. Surf. Sci.* **2019**, *479*, 963–973. [CrossRef]

132. Huang, H.; Tian, Y.; Xie, Y.; Mo, R.; Hu, J.; Li, M.; Sheng, X.; Jiang, X.; Zhang, X. Modification of graphene oxide with acrylate phosphorus monomer via thiol-Michael addition click reaction to enhance the anti-corrosive performance of waterborne epoxy coatings. *Prog. Org. Coat.* **2020**, *146*, 105724. [CrossRef]

133. Jin, T.; Xie, Z.; Fullston, D.; Huang, C.; Zeng, R.; Bai, R. Corrosion resistance of copolymerization of acrylamide and acrylic acid grafted graphene oxide composite coating on magnesium alloy. *Prog. Org. Coat.* **2019**, *136*, 105222. [CrossRef]

134. Harley, C.C.; Annibaldi, V.; Yu, T.; Breslin, C.B. The selective electrochemical sensing of dopamine at a polypyrrole film doped with an anionic β−cyclodextrin. *J. Electroanal. Chem.* **2019**, *855*, 113614. [CrossRef]

135. Carragher, U.; Breslin, C.B. Polypyrrole doped with dodecylbenzene sulfonate as a protective coating for copper. *Electrochim. Acta* **2018**, *291*, 362–372. [CrossRef]

136. Annibaldi, V.; Rooney, A.D.; Breslin, C.B. Corrosion protection of copper using polypyrrole electrosynthesised from a salicylate solution. *Corros. Sci.* **2012**, *59*, 179–185. [CrossRef]

137. Samanta, P.N.; Das, K.K. Deciphering the impact of surface defects and functionalization on the binding strength and electronic properties of graphene-polypyrrole nanocomposites: A first-principles approach. *J. Phys. Chem. C* **2019**, *123*, 5447–5459. [CrossRef]

138. Qiu, S.; Li, W.; Zheng, W.; Zhao, H.; Wang, L. Synergistic effect of polypyrrole-intercalated graphene for enhanced corrosion protection of aqueous coating in 3.5% NaCl solution. *ACS Appl. Mater. Interfaces* **2017**, *9*, 34294–34304. [CrossRef]

139. Zhu, Q.; Li, E.; Liu, X.; Song, W.; Li, Y.; Wang, X.; Liu, C. Epoxy coating with in-situ synthesis of polypyrrole functionalized graphene oxide for enhanced anticorrosive performance. *Prog. Org. Coat.* **2020**, *140*, 105488. [CrossRef]

140. Jiang, L.; Syed, J.A.; Lu, H.; Meng, X. In-situ electrodeposition of conductive polypyrrole-graphene oxide composite coating for corrosion protection of 304SS bipolar plates. *J. Alloys Compd.* **2019**, *770*, 35–47. [CrossRef]

141. Li, M.; Ji, X.; Cui, L.; Liu, J. In situ preparation of graphene/polypyrrole nanocomposite via electrochemical co-deposition methodology for anti-corrosion application. *J. Mater. Sci.* **2017**, *52*, 12251–12265. [CrossRef]

142. Merisalu, M.; Kahro, T.; Kozlova, J.; Niilisk, A.; Nikolajev, A.; Marandi, M.; Floren, A.; Alles, H.; Sammelselg, V. Graphene-polypyrrole thin hybrid corrosion resistant coatings for copper. *Synth. Met.* **2015**, *200*, 16–23. [CrossRef]

143. Jiang, L.; Syed, J.A.; Zhang, G.; Ma, Y.; Ma, J.; Lu, H.; Meng, X. Enhanced anticorrosion performance of PPY-graphene oxide/PPY-camphorsulfonic acid composite coating for 304SS bipolar plates in proton exchange membrane fuel cell. *J. Ind. Eng. Chem.* **2019**, *80*, 497–507. [CrossRef]

144. Jiang, S.; Liu, Z.; Jiang, D.; Cheng, H.; Han, J.; Han, S. Graphene as a nanotemplating auxiliary on the polypyrrole pigment for anticorrosion coatings. *High. Perform. Polym.* **2016**, *28*, 747–757. [CrossRef]

145. Bethencourt, M.; Botana, F.J.; Marcos, M.; Osuna, R.M.; Sánchez-Amaya, J.M. Inhibitor properties of "green" pigments for paints. *Prog. Org. Coat.* **2003**, *46*, 280–287. [CrossRef]

146. Zhu, Q.; Li, E.; Liu, X.; Song, W.; Zhao, M.; Zi, L.; Wang, X.; Liu, C. Synergistic effect of polypyrrole functionalized graphene oxide and zinc phosphate for enhanced anticorrosion performance of epoxy coatings. *Compos. Part A Appl. Sci. Manuf.* **2020**, *130*, 105752. [CrossRef]

147. Wang, H.; Hao, Q.; Yang, X.; Lu, L.; Wang, X. A nanostructured graphene/polyaniline hybrid material for supercapacitors. *Nanoscale* **2010**, *2*, 2164–2170. [CrossRef]

148. Yuan, T.H.; Zhang, Z.H.; Li, J.; Zhang, D.Q.; Gao, L.X.; Li, W.G.; Fan, Z.F. Corrosion protection of aluminum alloy by epoxy coatings containing polyaniline modified graphene additives. *Mater. Corros.* **2019**, *70*, 1298–1305. [CrossRef]

149. Harfouche, N.; Gospodinova, N.; Nessark, B.; Perrin, F.X. Electrodeposition of composite films of reduced graphene oxide/polyaniline in neutral aqueous solution on inert and oxidizable metal. *J. Electroanal. Chem.* **2017**, *786*, 135–144. [CrossRef]

150. Jin, T.; Zhang, Q.; Yin, H.; Cole, I.S.; Zhao, P.; Wang, Y.; Liu, X. Corrosion resistance of itaconic acid doped polyaniline/nanographene oxide composite coating. *Nanotechnology* **2020**, *31*, 285704. [CrossRef]

151. Hayatgheib, Y.; Ramezanzadeh, B.; Kardar, P.; Mahdavian, M. A comparative study on fabrication of a highly effective corrosion protective system based on graphene oxide-polyaniline nanofibers/epoxy composite. *Corros. Sci.* **2018**, *133*, 358–373. [CrossRef]

152. Lin, Y.-T.; Don, T.-M.; Wong, C.-J.; Meng, F.-C.; Lin, Y.-J.; Lee, S.-Y.; Lee, C.-F.; Chiu, W.-Y. Improvement of mechanical properties and anticorrosion performance of epoxy coatings by the introduction of polyaniline/graphene composite. *Surf. Coat. Technol.* **2019**, *374*, 1128–1138. [CrossRef]

153. Mooss, V.A.; Bhopale, A.A.; Deshpande, P.P.; Athawale, A.A. Graphene oxide-modified polyaniline pigment for epoxy based anti-corrosion coatings. *Chem. Pap.* **2017**, *71*, 1515–1528. [CrossRef]

154. Andreoli, E.; Annibaldi, V.; Rooney, D.A.; Breslin, C.B. Electrochemical fabrication of copper-based hybrid microstructures and mechanism of formation of related hierarchical structures on polypyrrole films. *J. Phys. Chem. C* **2011**, *115*, 20076–20083. [CrossRef]

155. Fazli-Shokouhi, S.; Nasirpouri, F.; Khatamian, M. Polyaniline-modified graphene oxide nanocomposites in epoxy coatings for enhancing the anticorrosion and antifouling properties. *J. Coat. Technol. Res.* **2019**, *16*, 983–997. [CrossRef]

156. Lei, Y.; Qiu, Z.; Liu, J.; Li, D.; Tan, N.; Liu, T.; Zhang, Y.; Chang, X.; Gu, Y.; Yin, Y. Effect of conducting polyaniline/graphene nanosheet content on the corrosion behavior of zinc-rich epoxy primers in 3.5% NaCl solution. *Polymers* **2019**, *11*, 850. [CrossRef]

157. Hao, Y.; Zhao, Y.; Li, B.; Song, L.; Guo, Z. Self-healing effect of graphene@PANI loaded with benzotriazole for carbon steel. *Corros. Sci.* **2020**, *163*, 108246. [CrossRef]

158. Zhong, F.; He, Y.; Wang, P.; Chen, C.; Yu, H.; Li, H.; Chen, J. Graphene/V_2O_5@polyaniline ternary composites enable waterborne epoxy coating with robust corrosion resistance. *React. Funct. Polym.* **2020**, *151*, 104567. [CrossRef]

159. Liu, J.; Lei, Y.; Qiu, Z.; Li, D.; Liu, T.; Zhang, F.; Sun, S.; Chang, X.; Fan, R.; Yin, Y. Insight into the impact of conducting polyaniline/graphene nanosheets on corrosion mechanism of zinc-rich epoxy primers on low alloy DH32 steel in artificial sea water. *J. Electrochem. Soc.* **2018**, *165*, C878–C889. [CrossRef]

160. Shen, L.; Li, Y.; Zhao, W.; Miao, L.; Xie, W.; Lu, H.; Wang, K. Corrosion protection of graphene-modified zinc-rich epoxy coatings in dilute NaCl Solution. *ACS Appl. Nano Mater.* **2019**, *2*, 180–190. [CrossRef]

161. Yang, N.; Yang, T.; Wang, W.; Chen, H.; Li, W. Polydopamine modified polyaniline-graphene oxide composite for enhancement of corrosion resistance. *J. Hazard. Mater.* **2019**, *377*, 142–151. [CrossRef]

162. Ye, Y.; Zhang, D.; Liu, T.; Liu, Z.; Pu, J.; Liu, W.; Zhao, H.; Li, X.; Wang, L. Superior corrosion resistance and self-healable epoxy coating pigmented with silanzied trianiline-intercalated graphene. *Carbon* **2019**, *142*, 164–176. [CrossRef]

163. Lu, H.; Zhang, S.; Zhao, Z.; Zhou, Y.; Li, W. Preparation and corrosion protection of VB_2 modified trimer aniline-reduced graphene oxide(VTA-rGO) coatings. *Prog. Org. Coat.* **2019**, *132*, 95–99. [CrossRef]

164. Ye, Y.; Yang, D.; Zhang, D.; Chen, H.; Zhao, H.; Li, X.; Wang, L. POSS-tetraaniline modified graphene for active corrosion protection of epoxy-based organic coating. *Chem. Eng. J.* **2020**, *383*, 123160. [CrossRef]

165. Gu, L.; Liu, S.; Zhao, H.; Yu, H. Facile Preparation of water-dispersible graphene sheets Stabilized by Carboxylated Oligoanilines and Their Anticorrosion Coatings. *ACS Appl. Mater. Interfaces* **2015**, *7*, 17641–17648. [CrossRef]

166. Rohwerder, M.; Michalik, A. Conducting polymers for corrosion protection: What makes the difference between failure and success? *Electrochim. Acta* **2007**, *53*, 1300–1313. [CrossRef]

167. Ryan, E.M.; Breslin, C.B. Formation of polypyrrole with dexamethasone as a dopant: Its cation and anion exchange properties. *J. Electroanal. Chem.* **2018**, *824*, 188–194. [CrossRef]

168. Deshpande, P.P.; Jadhav, N.G.; Gelling, V.J.; Sazou, D. Conducting polymers for corrosion protection: A review. *J. Coat. Technol. Res.* **2014**, *11*, 473–494. [CrossRef]

169. Batrakov, K.; Kuzhir, P.; Maksimenko, S.; Paddubskaya, A.; Voronovich, S.; Lambin, P.; Kaplas, T.; Svirko, Y. Flexible transparent graphene/polymer multilayers for efficient electromagnetic field absorption. *Sci. Rep.* **2014**, *4*, 7191. [CrossRef]

170. Fan, F.; Zhou, C.; Wang, X.; Szpunar, J. Layer-by-layer assembly of a self-healing anticorrosion coating on magnesium alloys. *ACS Appl. Mater. Interface* **2015**, *7*, 27271–27278. [CrossRef]

171. Zhang, J.; Zhang, W.; Wei, L.; Pu, L.; Liu, J.; Liu, H.; Li, Y.; Fan, J.; Ding, T.; Guo, Z. Alternating multilayer structural epoxy composite coating for corrosion protection of steel. *Macromol. Mater. Eng.* **2019**, *304*, 1900374. [CrossRef]

172. Yu, F.; Camilli, L.; Wang, T.; Makenzie, M.A.; Curioni, M.; Akid, R.; Bøggild, P. Complete long-term corrosion protection with chemical vapor deposited graphene. *Carbon* **2018**, *132*, 78–84. [CrossRef]

173. Gao, F.; Hu, Y.; Gong, Z.; Liu, T.; Gong, T.; Liu, S.; Zhang, C.; Quan, L.; Kaveendran, B.; Pan, C. Fabrication of chitosan/heparinized graphene oxide multilayer coating to improve corrosion resistance and biocompatibility of magnesium alloys. *Mater. Sci. Eng. C* **2019**, *104*, 109947. [CrossRef] [PubMed]

174. Hayatdavoudi, H.; Rahsepar, M. A mechanistic study of the enhanced cathodic protection performance of graphene-reinforced zinc rich nanocomposite coating for corrosion protection of carbon steel substrate. *J. Alloys Compd.* **2017**, *727*, 1148–1156. [CrossRef]

175. Kalendová, A.; Veselý, D.; Kohl, M.; Stejskal, J. Anticorrosion efficiency of zinc-filled epoxy coatings containing conducting polymers and pigments. *Prog. Org. Coat.* **2015**, *78*, 1–20. [CrossRef]

176. Teng, S.; Gao, Y.; Cao, F.; Kong, D.; Zheng, X.; Ma, X.; Zhi, L. Zinc-reduced graphene oxide for enhanced corrosion protection of zinc-rich epoxy coatings. *Prog. Org. Coat.* **2018**, *123*, 185–189. [CrossRef]

177. Liu, J.; Liu, T.; Guo, Z.; Guo, N.; Lei, Y.; Chang, X.; Yin, Y. Promoting barrier performance and cathodic protection of zinc-rich epoxy primer via single-layer graphene. *Polymers* **2018**, *10*, 591. [CrossRef]

178. Cao, X.; Huang, F.; Huang, C.; Liu, J.; Cheng, Y.F. Preparation of graphene nanoplate added zinc-rich epoxy coatings for enhanced sacrificial anode-based corrosion protection. *Corros. Sci.* **2019**, *159*, 108120. [CrossRef]

179. Ding, R.; Wang, X.; Jiang, J.; Gui, T.; Li, W. Study on evolution of coating state and role of graphene in graphene-modified low-zinc waterborne epoxy anticorrosion coating by electrochemical impedance spectroscopy. *J. Mater. Eng. Perform.* **2017**, *26*, 3319–3335. [CrossRef]

180. Huang, S.; Kong, G.; Yang, B.; Zhang, S.; Che, C. Effects of graphene on the corrosion evolution of zinc particles in waterborne epoxy zinc-containing coatings. *Prog. Org. Coat.* **2020**, *140*, 105531. [CrossRef]

181. Ge, T.; Zhao, W.; Wu, X.; Wu, Y.; Shen, L.; Ci, X.; He, Y. Design alternate epoxy-reduced graphene oxide/epoxy-zinc multilayer coatings for achieving long-term corrosion resistance for Cu. *Mater. Des.* **2020**, *186*, 108299. [CrossRef]

182. Taheri, N.N.; Ramezanzadeh, B.; Mahdavian, M. Application of layer-by-layer assembled graphene oxide nanosheets/polyaniline/zinc cations for construction of an effective epoxy coating anti-corrosion system. *J. Alloys Compd.* **2019**, *800*, 532–549. [CrossRef]

183. Cheng, L.; Liu, C.; Han, D.; Ma, S.; Guo, W.; Cai, H.; Wang, X. Effect of graphene on corrosion resistance of waterborne inorganic zinc-rich coatings. *J. Alloys Compd.* **2019**, *774*, 255–264. [CrossRef]

184. Ding, R.; Chen, S.; Zhou, N.; Zheng, Y.; Li, B.-J.; Gui, T.-J.; Wang, X.; Li, W.-H.; Yu, H.-B.; Tian, H.-W. The diffusion-dynamical and electrochemical effect mechanism of oriented magnetic graphene on zinc-rich coatings and the electrodynamics and quantum mechanics mechanism of electron conduction in graphene zinc-rich coatings. *J. Alloys Compd.* **2019**, *784*, 756–768. [CrossRef]

185. Wang, X.; Lv, J.; Ding, R.; Gui, T.-J.; Sun, M.-L. Application of EIS and transmission line model to study the effect of arrangement of graphene on electromagnetic shielding and cathodic protection performance of zinc-rich waterborne epoxy coatings. *Int. J. Electrochem. Sci.* **2020**, *15*, 4089–4101. [CrossRef]

186. Yang, B.; Zhang, P.; Wang, G.; Wang, A.; Chen, X.; Wei, S.; Xie, J. Effect of graphene oxide concentration in electrolyte on corrosion behavior of electrodeposited Zn-electrochemical reduction graphene composite coatings. *Coatings* **2019**, *9*, 758. [CrossRef]

187. Wu, H.; Zhang, L.; Liu, C.; Mai, Y.; Zhang, Y.; Jie, X. Deposition of Zn-G/Al composite coating with excellent cathodic protection on low-carbon steel by low-pressure cold spraying. *J. Alloy. Compd.* **2020**, *821*, 153483. [CrossRef]

188. Li, R.; Liang, J.; Hou, Y.; Chu, Q. Enhanced corrosion performance of Zn coating by incorporating graphene oxide electrodeposited from deep eutectic solvent. *RSC Adv.* **2015**, *5*, 60698–60707. [CrossRef]

189. Moshgi Asl, S.; Afshar, A.; Yaghoubinezhad, Y. An Electrochemical synthesis of reduced graphene oxide/zinc nanocomposite coating through pulse-potential electrodeposition technique and the consequent corrosion resistance. *Int. J. Corros.* **2018**, *2018*, 3028693. [CrossRef]

190. Karimi Azar, M.M.; Shooshtari Gugtapeh, H.; Rezaei, M. Evaluation of corrosion protection performance of electroplated zinc and zinc-graphene oxide nanocomposite coatings in air saturated 3.5 wt. % NaCl solution. *Colloids Surf. A Physicochem. Eng. Asp.* **2020**, *601*, 125051. [CrossRef]

191. Rekha, M.Y.; Srivastava, C. Microstructure and corrosion properties of zinc-graphene oxide composite coatings. *Corros. Sci.* **2019**, *152*, 234–248. [CrossRef]

192. Rekha, M.Y.; Kamboj, A.; Srivastava, C. Electrochemical behaviour of SnZn-graphene oxide composite coatings. *Thin Solid Film.* **2017**, *636*, 593–601. [CrossRef]

193. Rekha, M.Y.; Srivastava, C. Microstructural evolution and corrosion behavior of ZnNi-graphene oxide composite coatings. *Metall. Mater. Trans. A.* **2019**, *50*, 5896–5913. [CrossRef]

194. Wang, D.; Bierwagen, G.P. Sol-gel coatings on metals for corrosion protection. *Prog. Org. Coat.* **2009**, *64*, 327–338. [CrossRef]

195. Ciriminna, R.; Fidalgo, A.; Pandarus, V.; Béland, F.; Ilharco, L.M.; Pagliaro, M. The sol-gel route to advanced silica-based materials and recent applications. *Chem. Rev.* **2013**, *113*, 6592–6620. [CrossRef]

196. Zheng, S.; Li, J. Inorganic-organic sol gel hybrid coatings for corrosion protection of metals. *J. Sol. Gel Sci. Technol.* **2010**, *54*, 174–187. [CrossRef]

197. Ramezanzadeh, B.; Ahmadi, A.; Mahdavian, M. Enhancement of the corrosion protection performance and cathodic delamination resistance of epoxy coating through treatment of steel substrate by a novel nanometric sol-gel based silane composite film filled with functionalized graphene oxide nanosheets. *Corros. Sci.* **2016**, *109*, 182–205. [CrossRef]

198. Xue, B.; Yu, M.; Liu, J.; Liu, J.; Li, S.; Xiong, L. Corrosion protection of AA2024-T3 by sol-gel film modified with graphene oxide. *J. Alloys Compd.* **2017**, *725*, 84–95. [CrossRef]

199. Afsharimani, N.; Durán, A.; Galusek, D.; Castro, Y. Hybrid sol–gel silica coatings containing graphene nanosheets for improving the corrosion protection of AA2024-T3. *Nanomaterials* **2020**, *10*, 1050. [CrossRef]

200. Li, T.; Li, L.; Qi, J.; Chen, F. Corrosion protection of Ti6Al4V by a composite coating with a plasma electrolytic oxidation layer and sol-gel layer filled with graphene oxide. *Prog. Org. Coat.* **2020**, *144*, 105632. [CrossRef]

201. Yu, M.; Dong, H.; Shi, H.; Xiong, L.; He, C.; Liu, J.; Li, S. Effects of graphene oxide-filled sol-gel sealing on the corrosion resistance and paint adhesion of anodized aluminum. *Appl. Surf. Sci.* **2019**, *479*, 105–113. [CrossRef]

202. Parhizkar, N.; Ramezanzadeh, B.; Shahrabi, T. Enhancement of the corrosion protection properties of a hybrid sol-gel based silane film through impregnation of functionalized graphene oxide nanosheets. *J. Electrochem. Soc.* **2017**, *164*, C1044–C1058. [CrossRef]

203. Tian, S.; Liu, Z.; Shen, L.; Pu, J.; Liu, W.; Sun, X.; Li, Z. Performance evaluation of mercapto functional hybrid silica sol-gel coating and its synergistic effect with f-GNs for corrosion protection of copper surface. *RSC Adv.* **2018**, *8*, 7438–7449. [CrossRef]

204. Parhizkar, N.; Ramezanzadeh, B.; Shahrabi, T. Corrosion protection and adhesion properties of the epoxy coating applied on the steel substrate pre-treated by a sol-gel based silane coating filled with amino and isocyanate silane functionalized graphene oxide nanosheets. *Appl. Surf. Sci.* **2018**, *439*, 45–59. [CrossRef]

205. Xiong, L.; Liu, J.; Li, Y.; Li, S.; Yu, M. Enhancing corrosion protection properties of sol-gel coating by pH-responsive amino-silane functionalized graphene oxide-mesoporous silica nanosheets. *Prog. Org. Coat.* **2019**, *135*, 228–239. [CrossRef]

206. Xue, B.; Yu, M.; Liu, J.; Li, S.; Xiong, L.; Kong, X. Synthesis of inhibitor nanocontainers with two-dimensional structure and their anticorrosion action in sol-gel coating on AA2024-T3 aluminum alloy. *J. Electrochem. Soc.* **2017**, *164*, C641–C652. [CrossRef]

207. Maeztu, J.D.; Rivero, P.J.; Berlanga, C.; Bastidas, D.M.; Palacio, J.F.; Rodriguez, R. Effect of graphene oxide and fluorinated polymeric chains incorporated in a multilayered sol-gel nanocoating for the design of corrosion resistant and hydrophobic surfaces. *Appl. Surf. Sci.* **2017**, *419*, 138–149. [CrossRef]

208. Fernández-Hernán, J.P.; López, A.J.; Torres, B.; Rams, J. Silicon oxide multilayer coatings doped with carbon nanotubes and graphene nanoplatelets for corrosion protection of AZ31B magnesium alloy. *Prog. Org. Coat.* **2020**, *148*, 105836. [CrossRef]

209. Chen, M.; Huang, Z.; Liang, S.; Pei, F.; Lin, Z.; Dang, Z.; Wu, P. Immobilized Co^{2+} and Cu^{2+} induced structural change of layered double hydroxide for efficient heterogeneous degradation of antibiotic. *J. Hazard. Mater.* **2020**, *403*, 123554. [CrossRef]

210. Gong, M.; Li, Y.; Wang, H.; Liang, Y.; Wu, J.Z.; Zhou, J.; Wang, J.; Regier, T.; Wei, F.; Dai, H. An advanced Ni-Fe layered double hydroxide electrocatalyst for water oxidation. *J. Am. Chem. Soc.* **2013**, *135*, 8452–8455. [CrossRef]

211. Gao, Z.; Wang, J.; Li, Z.; Yang, W.; Wang, B.; Hou, M.; He, Y.; Liu, Q.; Mann, T.; Yang, P.; et al. Graphene nanosheet/Ni^{2+}/Al^{3+} layered double-hydroxide composite as a novel electrode for a supercapacitor. *Chem. Mater.* **2011**, *23*, 3509–3516. [CrossRef]

212. Zhang, F.; Zhao, L.; Chen, H.; Xu, S.; Evans, D.G.; Duan, X. Corrosion resistance of superhydrophobic layered double hydroxide films on aluminum. *Angew. Chem. Int. Ed.* **2008**, *47*, 2466–2469. [CrossRef]

213. Guo, X.; Xu, S.; Zhao, L.; Lu, W.; Zhang, F.; Evans, D.G.; Duan, X. One-step hydrothermal crystallization of a layered double hydroxide/alumina bilayer film on aluminum and its corrosion resistance properties. *Langmuir* **2009**, *25*, 9894–9897. [CrossRef] [PubMed]

214. Zhang, F.; Liu, Z.-G.; Zeng, R.-C.; Li, S.-Q.; Cui, H.-Z.; Song, L.; Han, E.-H. Corrosion resistance of Mg-Al-LDH coating on magnesium alloy AZ31. *Surf. Coat. Technol.* **2014**, *258*, 1152–1158. [CrossRef]

215. Zheludkevich, M.L.; Poznyak, S.K.; Rodrigues, L.M.; Raps, D.; Hack, T.; Dick, L.F.; Nunes, T.; Ferreira, M.G.S. Active protection coatings with layered double hydroxide nanocontainers of corrosion inhibitor. *Corros. Sci.* **2010**, *52*, 602–611. [CrossRef]

216. Tedim, J.; Poznyak, S.K.; Kuznetsova, A.; Raps, D.; Hack, T.; Zheludkevich, M.L.; Ferreira, M.G.S. Enhancement of active corrosion protection via combination of inhibitor-loaded nanocontainers. *ACS Appl. Mater. Interfaces* **2010**, *2*, 1528–1535. [CrossRef]

217. Du, P.; Wang, J.; Liu, G.; Zhao, H.; Wang, L. Facile synthesis of intelligent nanocomposites as encapsulation for materials protection. *Mater. Chem. Front.* **2019**, *3*, 321–330. [CrossRef]

218. Tedim, J.; Kuznetsova, A.; Salak, A.N.; Montemor, F.; Snihirova, D.; Pilz, M.; Zheludkevich, M.L.; Ferreira, M.G.S. Zn-Al layered double hydroxides as chloride nanotraps in active protective coatings. *Corros. Sci.* **2012**, *55*, 1–4. [CrossRef]

219. Yan, L.; Zhou, M.; Pang, X.; Gao, K. One-step in situ synthesis of reduced graphene oxide/Zn-Al layered double hydroxide film for enhanced corrosion protection of magnesium alloys. *Langmuir* **2019**, *35*, 6312–6320. [CrossRef]

220. Luo, X.; Yuan, S.; Pan, X.; Zhang, C.; Du, S.; Liu, Y. Synthesis and enhanced corrosion protection performance of reduced graphene oxide nanosheet/ZnAl layered double hydroxide composite films by hydrothermal continuous flow method. *ACS Appl. Mater. Interfaces* **2017**, *9*, 18263–18275. [CrossRef]

221. Zhang, Y.; Yu, P.; Wang, J.; Li, Y.; Chen, F.; Wei, K.; Zuo, Y. LDHs/graphene film on aluminum alloys for active protection. *Appl. Surf. Sci.* **2018**, *433*, 927–933. [CrossRef]

222. Yu, D.; Wen, S.; Yang, J.; Wang, J.; Chen, Y.; Luo, J.; Wu, Y. RGO modified ZnAl-LDH as epoxy nanostructure filler: A novel synthetic approach to anticorrosive waterborne coating. *Surf. Coat. Technol.* **2017**, *326*, 207–215. [CrossRef]

223. Zhao, Y.; Jiang, F.; Chen, Y.-Q.; Hu, J.-M. Coatings embedded with GO/MOFs nanocontainers having both active and passive protecting properties. *Corros. Sci.* **2020**, *168*, 108563. [CrossRef]

224. Ramezanzadeh, M.; Ramezanzadeh, B.; Mahdavian, M.; Bahlakeh, G. Development of metal-organic framework (MOF) decorated graphene oxide nanoplatforms for anti-corrosion epoxy coatings. *Carbon* **2020**, *161*, 231–251. [CrossRef]

225. Goncalves, G.; Marques, P.A.A.P.; Granadeiro, C.M.; Nogueira, H.I.S.; Singh, M.K.; Grácio, J. Surface modification of graphene nanosheets with gold nanoparticles: The role of oxygen moieties at graphene surface on gold nucleation and growth. *Chem. Mater.* **2009**, *21*, 4796–4802. [CrossRef]

226. Jin, J.; Zhang, L.; Shi, M.; Zhang, Y.; Wang, Q. Ti-GO-Ag nanocomposite: The effect of content level on the antimicrobial activity and cytotoxicity. *Int. J. Nanomed.* **2017**, *12*, 4209–4224. [CrossRef] [PubMed]

227. Liu, C.-S.; Liu, X.-C.; Wang, G.-C.; Liang, R.-P.; Qiu, J.-D. Preparation of nitrogen-doped graphene supporting Pt nanoparticles as a catalyst for oxygen reduction and methanol oxidation. *J. Electroanal. Chem.* **2014**, *728*, 41–50. [CrossRef]

228. Long, M.; Qin, Y.; Chen, C.; Guo, X.; Tan, B.; Cai, W. Origin of visible light photoactivity of reduced graphene oxide/TiO₂ by in situ hydrothermal growth of undergrown TiO₂ with graphene oxide. *J. Phys. Chem. C* **2013**, *117*, 16734–16741. [CrossRef]

229. Zhong, L.; Yun, K. Graphene oxide-modified ZnO particles: Synthesis, characterization, and antibacterial properties. *Int. J. Nanomed.* **2015**, *10*, 79–92. [CrossRef]

230. Boruah, P.K.; Sharma, B.; Karbhal, I.; Shelke, M.V.; Das, M.R. Ammonia-modified graphene sheets decorated with magnetic Fe₃O₄ nanoparticles for the photocatalytic and photo-Fenton degradation of phenolic compounds under sunlight irradiation. *J. Hazard. Mater.* **2017**, *325*, 90–100. [CrossRef]

231. Du, Y.J.; Damron, M.; Tang, G.; Zheng, H.; Chu, C.-J.; Osborne, J.H. Inorganic/organic hybrid coatings for aircraft aluminum alloy substrates. *Prog. Org. Coat.* **2001**, *41*, 226–232. [CrossRef]

232. Ma, Y.; Di, H.; Yu, Z.; Liang, L.; Lv, L.; Pan, Y.; Zhang, Y.; Yin, D. Fabrication of silica-decorated graphene oxide nanohybrids and the properties of composite epoxy coatings research. *Appl. Surf. Sci.* **2016**, *360*, 936–945. [CrossRef]

233. Song, B.; Shi, Y.; Liu, Q. An inorganic route to decorate graphene oxide with nanosilica and investigate its effect on anti-corrosion property of waterborne epoxy. *Polym. Adv. Technol.* **2020**, *31*, 309–318. [CrossRef]

234. Wang, T.; Ge, H.; Zhang, K. A novel core-shell silica@graphene straticulate structured antistatic anticorrosion composite coating. *J. Alloys Compd.* **2018**, *745*, 705–715. [CrossRef]

235. Bouibed, A.; Doufnoune, R. Synthesis and characterization of hybrid materials based on graphene oxide and silica nanoparticles and their effect on the corrosion protection properties of epoxy resin coatings. *J. Adhes. Sci. Technol.* **2019**, *33*, 834–860. [CrossRef]

236. Zhang, X.; Wen, J.; Hu, B.; Yuan, J.; Wang, J.; Zhu, L.; Pan, M. Dispersity control and anti-corrosive performance of graphene oxide modified by functionalized nanosilica in waterborne polyurethane. *Nanotechnology* **2020**, *31*, 205708. [CrossRef]

237. Shuai, C.; Wang, B.; Bin, S.; Peng, S.; Gao, C. Interfacial strengthening by reduced graphene oxide coated with MgO in biodegradable Mg composites. *Mater. Des.* **2020**, *191*, 108612. [CrossRef]

238. Palaniappan, N.; Cole, I.S.; Caballero-Briones, F.; Balasubaramanian, K.; Lal, C. Praseodymium-decorated graphene oxide as a corrosion inhibitor in acidic media for the magnesium AZ31 alloy. *RSC Adv.* **2018**, *8*, 34275–34286. [CrossRef]

239. Bakhsheshi-Rad, H.R.; Ismail, A.F.; Aziz, M.; Akbari, M.; Hadisi, Z.; Khoshnava, S.M.; Pagan, E.; Chen, X. Co-incorporation of graphene oxide/silver nanoparticle into poly-L-lactic acid fibrous: A route toward the development of cytocompatible and antibacterial coating layer on magnesium implants. *Mater. Sci. Eng. C* **2020**, *111*, 110812. [CrossRef]

240. Liu, Z.; Tian, S.; Li, Q.; Wang, J.; Pu, J.; Wang, G.; Zhao, W.; Feng, F.; Qin, J.; Ren, L. Integrated Dual-Functional ORMOSIL Coatings with AgNPs@rGO Nanocomposite for Corrosion Resistance and Antifouling Applications. *ACS Sustain. Chem. Eng.* **2020**, *8*, 6786–6797. [CrossRef]

241. Liu, J.; Yu, Q.; Yu, M.; Li, S.; Zhao, K.; Xue, B.; Zu, H. Silane modification of titanium dioxide-decorated graphene oxide nanocomposite for enhancing anticorrosion performance of epoxy coatings on AA-2024. *J. Alloys Compd.* **2018**, *744*, 728–739. [CrossRef]

242. Kavimani, V.; Prakash, K.S.; Gunashri, R.; Sathish, P. Corrosion protection behaviour of r-GO/TiO₂ hybrid composite coating on magnesium substrate in 3.5 wt.% NaCl. *Prog. Org. Coat.* **2018**, *125*, 358–364. [CrossRef]

243. Nazeer, A.A.; Al-Hetlani, E.; Amin, M.O.; Quiñones-Ruiz, T.; Lednev, I.K. A poly(butyl methacrylate)/graphene oxide/TiO₂ nanocomposite coating with superior corrosion protection for AZ31 alloy in chloride solution. *Chem. Eng. J.* **2019**, *361*, 485–498. [CrossRef]

244. Razavizadeh, O.; Ghorbani, M. Surface modification of carbon steel by ZnO-graphene nano-hybrid thin film. *Surf. Coat. Technol.* **2019**, *363*, 1–11. [CrossRef]

245. Othman, N.H.; Yahya, W.Z.N.; Che Ismail, M.; Mustapha, M.; Koi, Z.K. Highly dispersed graphene oxide–zinc oxide nanohybrids in epoxy coating with improved water barrier properties and corrosion resistance. *J. Coat. Technol. Res.* **2020**, *17*, 101–114. [CrossRef]

246. Tang, H.; Liu, Y.; Bian, D.; Guo, Y.; Zhao, Y. Fabrication of ZnO–GO hybrid for enhancement of chemically bonded phosphate ceramic coatings corrosion protection performance on AISI304L stainless steel. *Int. J. Appl. Ceram. Technol.* **2020**. [CrossRef]

247. Li, H.; Wang, J.; Yang, J.; Zhang, J.; Ding, H. Large CeO$_2$ nanoflakes modified by graphene as barriers in waterborne acrylic coatings and the improved anticorrosion performance. *Prog. Org. Coat.* **2020**, *143*, 105607. [CrossRef]

248. Arora, S.; Srivastava, C. Microstructure and corrosion properties of NiCo-graphene oxide composite coatings. *Thin Solid Film.* **2019**, *677*, 45–54. [CrossRef]

249. Yang, M.; Liu, B.; Xia, J.; Liu, Y.; Shi, Z.; Lv, X. Study on the properties of a novel electrostatic conductive and anti-corrosive composite coating improved by graphene nanosheets. *Prog. Org. Coat.* **2019**, *136*, 105244. [CrossRef]

250. Amrollahi, S.; Ramezanzadeh, B.; Yari, H.; Ramezanzadeh, M.; Mahdavian, M. In-situ growth of ceria nanoparticles on graphene oxide nanoplatelets to be used as a multifunctional (UV shield/radical scavenger/anticorrosive) hybrid compound for exterior coatings. *Prog. Org. Coat.* **2019**, *136*, 105241. [CrossRef]

251. Park, H.; Kim, K.Y.; Choi, W. Photoelectrochemical approach for metal corrosion prevention using a semiconductor photoanode. *J. Phys. Chem. B* **2002**, *106*, 4775–4781. [CrossRef]

252. Lu, X.; Liu, L.; Xie, X.; Cui, Y.; Oguzie, E.E.; Wang, F. Synergetic effect of graphene and Co(OH)$_2$ as cocatalysts of TiO$_2$ nanotubes for enhanced photogenerated cathodic protection. *J. Mater. Sci. Technol.* **2020**, *37*, 55–63. [CrossRef]

253. Li, H.; Wang, X.; Wei, Q.; Liu, X.; Qian, Z.; Hou, B. Enhanced photocathodic protection performance of Ag/graphene/TiO$_2$ composite for 304SS under visible light. *Nanotechnology* **2017**, *28*, 225701. [CrossRef] [PubMed]

254. Liu, W.; Du, T.; Ru, Q.; Zuo, S.; Cai, Y.; Yao, C. Preparation of graphene/WO$_3$/TiO$_2$ composite and its photocathodic protection performance for 304 stainless steel. *Mater. Res. Bull.* **2018**, *102*, 399–405. [CrossRef]

255. Yang, X.; Zhou, L.; Cao, G.; Song, Z.; Zhao, M. Fabrication of reduced graphene oxide wrapped TiO$_2$/SnO$_2$ photoanode and its anticorrosion property. *Optik* **2020**, *202*, 163573. [CrossRef]

256. Lv, R.; Robinson, J.A.; Schaak, R.E.; Sun, D.; Sun, Y.; Mallouk, T.E.; Terrones, M. Transition metal dichalcogenides and beyond: Synthesis, properties, and applications of single- and few-layer nanosheets. *Acc. Chem. Res.* **2015**, *48*, 56–64. [CrossRef]

257. Wang, Y.; Mayorga-Martinez, C.C.; Chia, X.; Sofer, Z.; Pumera, M. Nonconductive layered hexagonal boron nitride exfoliation by bipolar electrochemistry. *Nanoscale* **2018**, *10*, 7298–7303. [CrossRef]

258. Yi, M.; Shen, Z.; Zhao, X.; Liang, S.; Liu, L. Boron nitride nanosheets as oxygen-atom corrosion protective coatings. *Appl. Phys. Lett.* **2014**, *104*, 143101. [CrossRef]

259. Galbiati, M.; Stoot, A.C.; Mackenzie, D.M.A.; Bøggild, P.; Camilli, L. Real-time oxide evolution of copper protected by graphene and boron nitride barriers. *Sci. Rep.* **2017**, *7*, 39770. [CrossRef]

260. Cui, M.; Ren, S.; Zhang, G.; Liu, S.; Zhao, H.; Wang, L.; Xue, Q. Corrosion performance of hexagonal boron nitride doped waterborne epoxy coating. *J. Chin. Soc. Corros. Prot.* **2016**, *36*, 566–572. [CrossRef]

261. Zhao, H.; Ding, J.; Yu, H. The efficient exfoliation and dispersion of hBN nanoplatelets: Advanced application to waterborne anticorrosion coatings. *New J. Chem.* **2018**, *42*, 14433–14443. [CrossRef]

262. Li, L.H.; Xing, T.; Chen, Y.; Jones, R. Boron nitride nanosheets for metal protection. *Adv. Mater. Interfaces* **2014**, *1*, 1300132. [CrossRef]

263. Han, R.; Khan, M.H.; Angeloski, A.; Casillas, G.; Yoon, C.W.; Sun, X.; Huang, Z. Hexagonal boron nitride Nanosheets Grown via Chemical Vapor Deposition for Silver Protection. *ACS Appl. Nano Mater.* **2019**, *2*, 2830–2835. [CrossRef]

264. Jiang, H.; Wang, Z.; Ma, L.; Yang, Q.; Tang, Z.; Song, X.; Zeng, H.; Zhi, C. Boron ink assisted in situ boron nitride coatings for anti-oxidation and anti-corrosion applications. *Nanotechnology* **2019**, *30*, 335704. [CrossRef]

265. Cui, M.; Ren, S.; Chen, J.; Liu, S.; Zhang, G.; Zhao, H.; Wang, L.; Xue, Q. Anticorrosive performance of waterborne epoxy coatings containing water-dispersible hexagonal boron nitride (h-BN) nanosheets. *Appl. Surf. Sci.* **2017**, *397*, 77–86. [CrossRef]

266. Cui, M.; Ren, S.; Qin, S.; Xue, Q.; Zhao, H.; Wang, L. Processable poly(2-butylaniline)/hexagonal boron nitride nanohybrids for synergetic anticorrosive reinforcement of epoxy coating. *Corros. Sci.* **2018**, *131*, 187–198. [CrossRef]

267. Shi, H.; Liu, W.; Liu, C.; Yang, M.; Xie, Y.; Wang, S.; Zhang, F.; Liang, L.; Pi, K. Polyethylenimine-assisted exfoliation of h-BN in aqueous media for anticorrosive reinforcement of waterborne epoxy coating. *Prog. Org. Coat.* **2020**, *142*, 105591. [CrossRef]

268. Zhang, C.; He, Y.; Zhan, Y.; Zhang, L.; Shi, H.; Xu, Z. Poly(dopamine) assisted epoxy functionalization of hexagonal boron nitride for enhancement of epoxy resin anticorrosion performance. *Polym. Adv. Technol.* **2017**, *28*, 214–221. [CrossRef]

269. Cui, M.; Ren, S.; Qin, S.; Xue, Q.; Zhao, H.; Wang, L. Non-covalent functionalized hexagonal boron nitride nanoplatelets to improve corrosion and wear resistance of epoxy coatings. *RSC Adv.* **2017**, *7*, 44043–44053. [CrossRef]

270. Yu, J.; Zhao, W.; Liu, G.; Wu, Y.; Wang, D. Anti-corrosion mechanism of 2D nanosheet materials in waterborne epoxy coatings. *Surf. Topogr. Metrol. Prop.* **2018**, *6*, 034019. [CrossRef]

271. Zhang, C.; He, Y.; Li, F.; Di, H.; Zhang, L.; Zhan, Y. h-BN decorated with Fe_3O_4 nanoparticles through mussel-inspired chemistry of dopamine for reinforcing anticorrosion performance of epoxy coatings. *J. Alloys Compd.* **2016**, *685*, 743–751. [CrossRef]

272. Wan, P.; Zhao, N.; Qi, F.; Zhang, B.; Xiong, H.; Yuan, H.; Liao, B.; Ouyang, X. Synthesis of PDA-BN@f-Al_2O_3 hybrid for nanocomposite epoxy coating with superior corrosion protective properties. *Prog. Org. Coat.* **2020**, *146*, 105713. [CrossRef]

273. Wu, Y.; Yu, J.; Zhao, W.; Wang, C.; Wu, B.; Lu, G. Investigating the anti-corrosion behaviors of the waterborne epoxy composite coatings with barrier and inhibition roles on mild steel. *Prog. Org. Coat.* **2019**, *133*, 8–18. [CrossRef]

274. Husain, E.; Narayanan, T.N.; Taha-Tijerina, J.J.; Vinod, S.; Vajtai, R.; Ajayan, P.M. Marine corrosion protective coatings of hexagonal boron nitride thin films on stainless steel. *ACS Appl. Mater. Interfaces* **2013**, *5*, 4129–4135. [CrossRef]

275. Sun, W.; Wang, L.; Wu, T.; Pan, Y.; Liu, G. Communication—Multi-layer boron nitride nanosheets as corrosion-protective coating fillers. *J. Electrochem. Soc.* **2016**, *163*, C16–C18. [CrossRef]

276. Wang, Y.; Wang, X.; Antonietti, M. Polymeric graphitic carbon nitride as a heterogeneous organocatalyst: From photochemistry to multipurpose catalysis to sustainable chemistry. *Angew. Chem.* **2012**, *51*, 68–89. [CrossRef]

277. Yang, G.; Chen, T.; Feng, B.; Weng, J.; Duan, K.; Wang, J.; Lu, X. Improved corrosion resistance and biocompatibility of biodegradable magnesium alloy by coating graphite carbon nitride (g-C_3N_4). *J. Alloys Compd.* **2019**, *770*, 823–830. [CrossRef]

278. Kumar, A.M.; Khan, A.; Khan, M.Y.; Suleiman, R.K.; Jose, J.; Dafalla, H. Hierarchical graphitic carbon nitride-ZnO nanocomposite: Viable reinforcement for the improved corrosion resistant behavior of organic coatings. *Mater. Chem. Phys.* **2020**, *251*, 122987. [CrossRef]

279. Karimi, M.A.; Haji Aghaei, V.; Nezhadali, A.; Ajami, N. Investigation of copper corrosion in sodium chloride solution by using a new coating of polystyrene/g-C_3N_4. *J. Mater. Sci. Mater. Electron.* **2019**, *30*, 6300–6310. [CrossRef]

280. Zuo, S.; Chen, Y.; Liu, W.; Yao, C.; Li, Y.; Ma, J.; Kong, Y.; Mao, H.; Li, Z.; Fu, Y. Polyaniline/g-C_3N_4 composites as novel media for anticorrosion coatings. *J. Coat. Technol. Res.* **2017**, *14*, 1307–1314. [CrossRef]

281. Malav, J.K.; Rathod, R.; Umare, S.; Vidyasagar, D. Structural, thermal and anticorrosion properties of electroactive polyimide/gC_3N_4 composites. *Mater. Res. Express.* **2018**, *5*, 095309. [CrossRef]

282. Kumar, A.M.; Khan, M.Y.; Suleiman, R.K.; Khan, A.; Dafalla, H. Promising graphitic carbon nitride/MoO_x nanocomposites: For surface protective performance of AA2024 alloys in marine environment. *Surf. Coat. Technol.* **2019**, *374*, 579–590. [CrossRef]

283. Peng, Y.; Wang, L.; Liu, Y.; Chen, H.; Lei, J.; Zhang, J. Visible-light-driven photocatalytic H_2O_2 production on g-C_3N_4 loaded with CoP as a noble metal free cocatalyst. *Eur. J. Inorg. Chem.* **2017**, *2017*, 4797–4802. [CrossRef]

284. Haider, Z.; Cho, H.-I.; Moon, G.-H.; Kim, H.-I. Minireview: Selective production of hydrogen peroxide as a clean oxidant over structurally tailored carbon nitride photocatalysts. *Catal. Today* **2019**, *335*, 55–64. [CrossRef]

285. Zhang, X.; Chen, G.; Li, W.; Wu, D. Graphitic carbon nitride homojunction films for photocathodic protection of 316 stainless steel and Q235 carbon steel. *J. Electroanal. Chem.* **2020**, *857*, 113703. [CrossRef]